# Air-Water Partitioning of Biomass Burning Phenols and the Effects of Temperature and Salinity

Alexander S. McFall, Alex W. Johnson and Cort Anastasio\*

Department of Land, Air, and Water Resources

University of California Davis

Davis, CA 95670

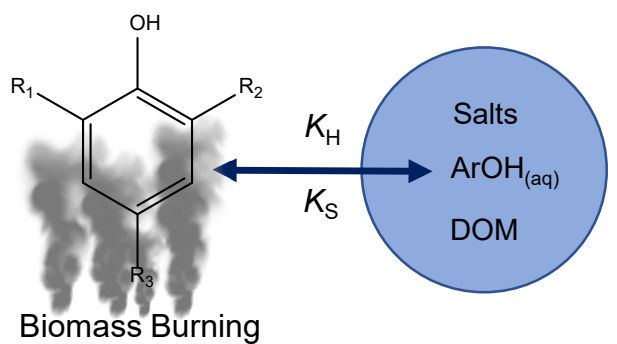
Submitted to Environmental Science and Technology: 25 October 2019

Revised Version Submitted: 13 January 2020

2<sup>nd</sup> Revision Submitted: ?Date?

Word Count: 4453 + 1800 (Figures) = 6253

# 2 TOC Abstract Art



3

#### 4 ABSTRACT

Biomass burning (BB) emits organic gases that, with chemical aging, can form secondary organic aerosol (SOA) in both the gas and aqueous phases. One class of biomass-burning emissions, phenols, are of interest because they react rapidly in the aqueous phase to efficiently form SOA, which might affect climate and human health. However, while measurements exist for the airwater partitioning constants of some simple phenols, Henry's law constants ( $K_H$ ) are unknown for more complex BB phenols. In this work, we use a custom-built apparatus to measure  $K_H$  for a suite of biomass-burning phenols that span a wide range of air-water partitioning coefficients. Comparing our measurements to predicted values from EPI Suite shows that this model consistently overestimates  $K_H$  unless a suitable measured phenol  $K_H$  value is included to adjust the calculations. In addition, we determine the effect of five salts on phenol partitioning by measuring the Setschenow coefficients ( $K_S$ ). Across the eight phenols we examined, values of  $K_S$  depend primarily on salt identity and descend in the order ( $N_{H_2} > N_4 > N$ 

#### INTRODUCTION

Emissions from biomass burning (BB) are significant contributors to particulate matter, accounting for 59% of black carbon and 85% of primary organic aerosol (POA) global emissions. In addition to these direct emissions of particles, volatile organic carbon (VOC) compounds from BB can undergo atmospheric aging to form secondary organic aerosol (SOA). SOA contributes significantly to total particle mass, impacts the global energy balance, and can cause health issues upon inhalation. Phenols emitted from biomass-burning are of particular interest due to their

potentially significant contributions to SOA mass. Gas-phase phenols are abundant in BB plumes, with emissions that are approximately 30 – 50% of the total mass of fine PM emitted.<sup>5</sup> The emitted phenols can be rapidly oxidized in the gas phase as well as in the aqueous phase, where oxidants such as triplet excited states of organic carbon ( $^{3}C^{*}$ ) and hydroxyl radical form aqSOA with mass yields near 100%. $^{6-10}$  While phenols can be oxidized in both phases, understanding the relative importance of the two broad paths requires knowing the air-water partitioning of phenols.

The Henry's law constant ( $K_H$ ) describes the equilibrium air-water partitioning of a species for dilute aqueous conditions (e.g., cloud and fog drops, surface waters). In the atmospheric literature,  $K_H$  is often presented as

where P is the partial pressure (atm) of the compound of interest and  $C_{aq}$  is the aqueous

$$K_H = \frac{c_{aq}}{P} \qquad (1)$$

concentration (M). While significant amounts of  $K_{\rm H}$  data exist for broad ranges of compounds, there are relatively few measurements for phenols and almost no data for phenols with high  $K_{\rm H}$  values. At a modest cloud or fog liquid water content ( $10^{-7}$  L<sub>aq</sub> L<sub>gas</sub>-1, i.e., 0.1 g-H<sub>2</sub>O m<sup>-3</sup>-air), a Henry's law constant of  $5\times10^4$  M atm<sup>-1</sup> is required for 10% of a compound to be present in the aqueous phase. At a  $K_{\rm H}$  value of value of  $4\times10^6$  M atm<sup>-1</sup>, 90% of the compound will be present in the aqueous phase.

In cases where Henry's law constants have not been measured, values can be estimated using models such as the EPI Suite HENRYWIN program from the U.S. Environmental Protection Agency. HENRYWIN uses quantitative structure-activity relationships (QSARs) to determine  $K_{\rm H}$  via bond or group contribution methods. He model can also apply measured  $K_{\rm H}$  data from core structures to its bond method calculations to determine an improved, Experimental

Value Adjusted (EVA) Henry's law constant. However, because of a lack of experimental data,

it is unclear whether the EPI-predicted Henry's law constants are reasonable for phenols with

50 high  $K_{\rm H}$  values.

49

52

53

54

55

56

58

63

64

65

66

67

68

69

51 Compared to dilute aqueous fog and cloud drops, partitioning into (and reactions in) aerosol

liquid water (ALW) will likely be different because of high concentrations of salts and other

solutes. Common inorganic salts include sodium chloride from sea spray, ammonium nitrate

from NO<sub>x</sub> emissions, and ammonium sulfate from SO<sub>2</sub> emissions, with other salts present in

smaller quantities. 17-19 With a lower liquid water content, the extent of partitioning into ALW is

generally reduced relative to a cloud or fog. For example, even ignoring the impacts of salts,

under wet ALW conditions (100  $\mu$ g H<sub>2</sub>O m<sup>-3</sup>)  $K_{\rm H}$  values of 5 × 10<sup>4</sup> and 4 × 10<sup>6</sup> M atm<sup>-1</sup>

correspond to aqueous fractions of only 0.01% and 0.9%, respectively.

In addition, the higher salt and solute content of ALW can alter gas-aqueous partitioning, as

described by the Setschenow relation:<sup>20, 21</sup>

$$\log(K_{\frac{1}{\text{salt}}}/K_{\frac{1}{\text{water}}}) = K_S C_{salt} (2)$$

where  $K_{1/\text{salt}}$  and  $K_{1/\text{water}}$  are partitioning coefficients of a compound between a non-aqueous

phase 1 (e.g., the gas phase) and a salt solution of concentration  $C_{salt}$  (M) or water (i.e., no salt),

and  $K_S$  is the Setschenow constant (M<sup>-1</sup>). When  $K_S$  is positive, the compound of interest is

"salted-out" of aqueous solution, i.e., it has a stronger tendency to partition out of solution as the

salt concentration increases. This decrease in effective  $K_{\rm H}$ , will decrease the aqueous

concentration below what is predicted via simple partitioning using only  $K_{\rm H}$ . Recent work

indicates that the presence of salts affects more than just the aqueous concentrations of aerosol

constituents. For example, photochemical reaction rates of both acetosyringone and pyruvic acid,

common in organic aerosols, increased in the presence of inorganic salts.<sup>22, 23</sup> Salt identity also plays an important role, altering the extent of partitioning for a range of organic compounds.<sup>24, 25</sup> In this work, we first experimentally determine  $K_{\rm H}$  for a suite of biomass-burning phenols spanning a wide range of values and compare them with values predicted by EPI Suite. We also determine the dependence of  $K_{\rm H}$  on temperature for three phenols and compare our resulting  $\Delta H_{\rm sol}$  measurements to literature values for other phenols. We next measure values of  $K_{\rm S}$  for each of our phenols in five different salts to determine the effects of salt concentration and identity on partitioning. Lastly, we combine our  $K_{\rm H}$  and  $K_{\rm S}$  results to describe the air-water partitioning of biomass-burning phenols in dilute aqueous and in particle water conditions and discuss the implications for atmospheric processing of phenols.

#### MATERIALS AND METHODS

81 Chemicals

70

71

72

73

74

75

76

77

78

79

- 82 Vanillyl alcohol (VanOH, >98%), vanillyl ethyl ether (VanEth, >98%), 4-propylguaiacol
- 83 (PropGua,  $\geq 99\%$ ), zingerone (Zing,  $\geq 98\%$ ), guaiacylacetone (GA, 96%), guaiacol (Gua,  $\geq 98\%$ ),
- 84 eugenol (Eug, 99%), and ethylenediaminetetraacetic acid (EDTA, >99.995%) were purchased
- from Sigma Aldrich. Syringylacetone (SA, 82%) was synthesized by Carbosynth LLC.
- 86 Methanol, acetonitrile, and water used in sample extraction and XAD-4 preparation were Optima
- 87 LC-MS grade from Fisher Scientific. Reservoir solutions were prepared in ultrapure Milli-Q
- water (18.2 M $\Omega$  cm) from a Millipore Advantage A10 system with upstream organic filter
- 89 (Barnstead).

## Henry's Law Determination

The custom-built equilibrium partitioning system used to determine Henry's law constants is based on the  $K_H$  system of Fendinger and Glotfelty,  $^{26}$  and is described in section S1 of the Supporting Information. Briefly, a metered, purified, humidified, temperature-controlled  $N_2$  flow is passed into a temperature-controlled wetted wall column lined with glass fiber filter and supplied with a constant flow of phenol solution. The phenol reaches equilibrium air-water partitioning in the column and the gas-phase phenol in the  $N_2$  flow exiting the column is collected onto a downstream plug of clean XAD-4 resin (Figure S1).

Collecting the gas flow for varying amounts of time allows us to calculate the delivery rate of gas-phase phenol,  $R_g$  (mol min<sup>-1</sup>). A typical example of our experimental data is included in Figure S4 of the Supporting Information. Using the experimental flow rate and assuming ideal gas behavior, we solve for the partial pressure of the phenol in the gas stream ( $P_{ArOH}$ , atm):

$$P_{ArOH} = \frac{R_g N_A}{O n_o} \times P_{tot}$$
 (3)

where  $N_A$  is Avogadro's number, Q is the experimental flow rate in cm<sup>3</sup> min<sup>-1</sup>,  $P_{\text{tot}}$  is the total atmospheric pressure in atm, and  $n_\theta$  is the total gas concentration adjusted for the experimental temperature (e.g.,  $2.46 \times 10^{19}$  mlc cm<sup>-3</sup> at 298 K and 1 atm). Over the period of data collection, the average ( $\pm 1\sigma$ ) atmospheric pressure was  $1.00 \pm 0.02$  atm, as recorded in the Davis campus weather data archive (http://atm.ucdavis.edu/weather/uc-davis-weather-climate-station/). Thus, we use 1.00 atm for  $P_{\text{tot}}$  for all experiments and do not adjust for the very small daily changes. Before the gas-phase flow is collected in a given experiment, the system is conditioned by running the phenol solution and  $N_2$  until phenol no longer adsorbs to inner surfaces of the

system. For each experiment we also measure phenol concentrations in the reservoirs above and below the column to ensure no significant degradation of phenol occurred on the filter surface. Experiments are also accompanied by periodic XAD resin blanks to ensure no background contamination, and daily matrix spikes to determine experimental recoveries of each phenol from the resin. Recoveries are tabulated in Table S1 of the Supplement. All samples, with the exception of syringylacetone, are shake extracted for 30 minutes using 30 mL of acetonitrile. Samples of syringylacetone are extracted in 30 mL of 35:65 acetonitrile:water mixture to avoid a final dilution. To test that one tube of XAD is sufficient to collect all of the gas-phase phenol, two collection tubes are attached in series for initial experiments with each phenol. Extraction of the separate tubes confirmed that no phenol is detectable in the second tube at the longest collection times.

Determination of  $K_H$  for most compounds is accomplished within a single experimental day, with a 3-hour system conditioning time and a longest collection time-point of 2 hours. However, for samples of vanillyl alcohol and syringylacetone, where expected gas-phase concentrations are very low, 24 hours of equilibration time is used. The maximum collection time for these samples is also 24 hours, and the gas flow rate is increased to 500 mL min<sup>-1</sup> and 600 mL min<sup>-1</sup> for VanOH and SA, respectively. These conditions ensure adequate delivery of both compounds for extraction and analysis. In future work, we recommend that replicates of higher- $K_H$  compounds like SA are paired with a suitable concentration step to reduce collection times, and glassware is end-capped to reduce system conditioning time. All experiments are performed in a minimum of triplicate except for SA, for which the reported value is a single determination ( $\pm$  standard error) due to a scarcity of compound.

#### LC-MS Analysis

Samples for both  $K_H$  and  $K_S$  are analyzed using an Agilent 1260 Infinity series HPLC coupled to an Agilent 6420 quadrupole mass spectrometer with an electrospray ionization (ESI) source in positive mode. For  $K_H$  samples, the stationary phase is an Agilent Poroshell 120 PFP column (50  $\times$  2.7 mm) and the mobile phase is an isocratic mixture of 35:65 acetonitrile and water. For  $K_S$  samples, the stationary phase is a Thermo Scientific BetaBasic C18 column (250  $\times$  3 mm), and the mobile phase is an isocratic mixture of 40:60 acetonitrile and water. Detailed chromatographic and ion source conditions are provided in Tables S2a and S2b.

#### Setschenow Determination

The Setschenow coefficient describes the impact of salt on the partitioning of a compound between two phases. In this work, we use the non-depletion solid phase micro extraction (SPME) method of Endo et al.<sup>27</sup> For our study, a 1.5 cm length of polyacrylate (PA)-coated SPME fiber (Polymicro Technologies, 360 µm diameter, 97 µm coating thickness) is added to a 20 mL amber scintillation vial containing 15 mL of a known concentration (0.1 -1 mM) of aqueous phenol (or a mixture thereof) and salt. We tested the impact of five salts (ammonium nitrate, potassium nitrate, sodium chloride, ammonium chloride, and ammonium sulfate) at range of salt concentrations from no salt to a maximum of 3 M (except for potassium nitrate (2.7 M) and ammonium nitrate (5.75 M)). Typical experiments mix at least three phenols at individual concentrations of 0.5 mM each, spiked into triplicate vials of five salt concentrations (i.e., 15 samples per salt experiment). We usually measure four salts per experiment, accompanied by three fiber blanks (water only, no phenol) for a total of 63 samples. We cap and foil cover the vials before placing them in secure racks on a shake table. The samples are shaken for 48 hours,

which was the amount of time necessary for the fiber concentration of each phenol to plateau in initial testing. Once equilibrated, fibers are wiped with dry tissue and added to autosampler vials with 1.5 mL of acetonitrile for a 10-minute shake extraction. Sequential extractions of the fibers showed no remaining phenol on the fiber after the first extraction. A 400  $\mu$ L aliquot of extract is added to 600  $\mu$ L of water (Optima grade) for final analysis using the LC/MS method described above. Phenol concentrations are measured in each SPME extract and  $K_S$  is determined as the linear regression slope of a plot of log ( $C_S/C_W$ ) versus salt concentration:

$$\frac{\Delta \log(\frac{C_S}{C_W})}{\Delta C_{Salt}} = K_S \tag{4}$$

where  $C_s$  and  $C_w$  are the concentrations in the saltwater and pure water fiber extracts, respectively. Experiments were performed in a minimum of triplicate and all data was combined to determine  $K_S$  from a single regression for a given phenol and salt. A few examples of our experimental data are shown in Figure S5. Corresponding hydrolysis controls (i.e., phenol solution with no salt and no fiber) accompanied each experiment to account for any phenol hydrolysis, which was below 5 percent. Additional controls with the addition of 10  $\mu$ M EDTA confirmed that any trace metals in our salts do not affect  $K_S$  partitioning. Using the mass of phenol extracted from each SPME fiber (and the total mass of phenol present in each sample with the highest salt concentration), we check that mass depletion from solution to fiber for each salt and phenol combination is negligible.

#### **RESULTS AND DISCUSSION**

Henry's Law Constants and Comparison to Predicted Values

178

179

197

198

199

180 As described in the Supporting Information, we validated our wetted wall system by measuring the Henry's law constant for guaiacol, a significant product from biomass burning.<sup>5</sup> Our guaiacol 181  $K_{\rm H}$  value ( $\pm 1\sigma$ ) at 298 K,  $878 \pm 38$  M atm<sup>-1</sup>, matched previous literature determinations.<sup>28</sup> To 182 build on this work, here we study seven additional biomass-burning phenols, shown in Figure 1.5 183 184 Our tested phenols share the common guaiacyl (1-hydroxy-2-methoxyphenyl) and syringyl (1-185 hydroxy-2,6-dimethoxyphenyl) base structures with varying functional groups at the para 186 position. Guaiacyl structures are common in both hardwood and softwood smoke emissions, while syringyl structures are more commonly associated with hardwood burning.<sup>5</sup> 187 Our measured  $K_{\rm H}$  values for these seven phenols range from  $10^2$  to  $10^8$  M atm<sup>-1</sup> at 298 K (Table 188 189 S4), representing a very wide range of air-water partitioning. As discussed later, for this range of values, the aqueous fraction for a typical cloud (liquid water content 0.1 g m<sup>-3</sup>) ranges from less 190 191 than 1% (e.g., guaiacol, 4-propylguaiacol, eugenol) to near 100% (guaiacylacetone, vanillyl 192 alcohol, syringylacetone). As the degree of para-chain functionalization increases with the 193 addition of ketone or alcohol groups, the degree of partitioning increases substantially, likely due 194 to increases in overall molecular polarity and decreased volatility. Figure 2 summarizes the relationship between the EPI Suite predicted values and our 195 196 measurements, both at 298 K. The top panel (Figure 2a) displays predicted data using the EPI

Suite bond method. This methodology uses known K<sub>H</sub> values to determine the contributions of

individual chemical bonds to  $K_{\rm H}$ , and applies these contributions to predict unknown values of

 $K_{\rm H}$ . This bond method overestimates  $K_{\rm H}$  for every phenol tested, with a ratio of predicted to

measured values ranging from 2 to 280 and an average ratio of 54 (Figure 2A and Table S4). These significant prediction problems can lead to large errors in the calculated fraction of the phenol that is in the aqueous phase, which alters aqueous rates and processes. For example, at a typical cloud liquid water content of  $10^{-7}$   $L_{aq}$   $L_{air}^{-1}$ , the predicted value for VanEth yields an aqueous fraction of 74 % at 298 K, while the actual measured value yields an aqueous fraction of 9%.

200

201

202

203

204

205

206

207

208

209

210

211

212

213

214

215

216

217

218

219

220

221

222

However, when we use the Experimental Value Adjustment (EVA) method, EPI Suite's calculation agrees very well with our experimental determinations (Figure 2b). We use methylguaiacol, guaiacol, and syringol as base structures with known  $K_{\rm H}$  values to refine the EPI calculations. Using EVA, the ratio of predicted to measured values of K<sub>H</sub> is much better, with an average of 0.94 and a range of 0.05 (syringylacetone) to 2.1 (vanillyl alcohol) (Figure 2b and Table S4). Clearly, including the basic guaiacol and syringol structures can greatly increase the accuracy of air-water partitioning predictions. However, we note that use of phenol in EVA calculations, which should act as the simplest base structure for our suite of compounds, gives far worse results than the closer guaiacol and syringol base structures. We consider guaiacol as a test case; the EPI Suite experimental database lists phenol as  $3\times10^3$  M atm<sup>-1</sup> at 298 K and yields an EVA calculated value of  $5.1 \times 10^4$  M atm<sup>-1</sup> for guaiacol, 58-fold higher than the true value. Though there has been some discrepancy in measurements of the physical properties of phenol,<sup>29</sup> we select the value of Feigenbrugel et al. (501 M atm<sup>-1</sup> at 298 K) to represent the phenol K<sub>H</sub> measurement and refine our EVA calculations.<sup>30</sup> Based upon review of other works using different measurement systems (e.g., gas-stripping columns in Harrison et al., static equilibrium from Sheikheldin et al.), 31, 32 we have selected the data of Feigenbrugel et al. because the work covers a wider combined range of experimental phenol concentrations, gas flow rates, and

temperatures. In addition, the agreement between data collections under these different conditions suggests that phase equilibrium was properly achieved within their system. Repeating our EVA analysis of guaiacol with this value improves the prediction to a 10-fold overestimation  $(K_{\rm H}=8.5\times10^3~{\rm M~atm^{-1}})$ . Though phenol presents some problems as a predictor, the addition of experimental data for more substituted structures, such as the results of this work, should help predictions for even more complicated phenol structures. Towards this goal, in Table S5 we list Henry's law constants for the nearly 40 phenols identified from wood combustion by Schauer et al.<sup>5</sup> determined using a combination of past  $K_{\rm H}$  measurements, our new measurements, and new predictions from the EVA method.

Equation 5 describes the relationship between the EVA predicted and our measured values from Figure 2B:

$$\log K_{Predicted} = (0.895 \pm 0.088) \times \log K_{Measured} + (0.359 \pm 0.476)$$
 (5)

- where  $K_{Predicted}$  and  $K_{Measured}$  are the predicted and measured Henry's law constants (M atm<sup>-1</sup>).
- The correlation of this relationship is quite good ( $R^2 = 0.945$ ), indicating that EPI Suite with the
- proper EVA base structure is a robust method for predicting  $K_{\rm H}$  values for phenols.
- 238 Effect of Temperature

223

224

225

226

227

228

229

230

- We examined the temperature dependence of  $K_{\rm H}$  for three compounds guaiacylacetone, vanillyl
- 240 ethyl ether, and zingerone. Relationships with temperature are expressed in van't Hoff form:

$$\ln(K_H) = -\frac{\Delta H_{sol}}{R} \times \frac{1}{T} + \frac{\Delta S}{R} \quad (6)$$

where  $\Delta H_{\rm sol}$  is the enthalpy of solvation, R is the gas constant (J mol<sup>-1</sup> K<sup>-1</sup>), T is the temperature (K), and  $\Delta S$  is the entropy (J K<sup>-1</sup>). The van't Hoff plots of the three phenols are shown in Figure 3. Based on the slopes from these plots, the enthalpies of solvation,  $\Delta H_{\rm sol}$  (kJ mol<sup>-1</sup>) are ( $-70 \pm 5$ ) for GA, ( $-85 \pm 12$ ) for Zing, and ( $-112\pm 7$ ) for VanEth (Table S5). Previously measured enthalpies for other substituted phenols range from -52 to -77 kJ mol<sup>-1</sup> (Figure S6).<sup>28, 30, 33</sup> While our  $\Delta H_{\rm sol}$  values for GA and Zing are not significantly different from those of previously measured phenols, VanEth has a much larger value. Excluding VanEth, the measured phenols yield a relatively consistent average  $\Delta H_{\rm sol}$  value ( $\pm 1\sigma$ ) of  $-65 \pm 9$  kJ mol<sup>-1</sup>. In addition, we find no relationship between  $K_{\rm H}$  and  $\Delta H_{\rm sol}$  (Figure S7).

Structural differences may be responsible for the observed differences in dissolution enthalpy between VanEth and the other phenols. GA, Zing, and VanEth are all guaiacol base structures with different chain functionalization at the para position (Figure 1). GA and Zing, which contain acetone and butanone substituents, respectively, have similar enthalpies that are at the upper end of literature  $\Delta H_{\rm sol}$  values for phenols such as guaiacol,<sup>28</sup> phenol,<sup>30</sup> and 2-ethylphenol.<sup>34</sup> In contrast, VanEth, which contains a methyl-ethyl ether substituent, exhibits a stronger dependence on temperature than the other phenols, although the reasons for this are unclear.

#### Setschenow Coefficients

We next examine the effect of salinity on the partitioning of each phenol. Since the Setschenow relation gives the salt effect relative to any second phase, our fiber-saltwater partitioning experiments measure the same effect that will occur in gas-aqueous partitioning with dissolved salts. As shown in Figure S5, the aqueous-SPME partitioning decreases (i.e., less phenol is present in the solution at equilibrium) as the amount of salt increases. In general, only 0.1% to

1% of the initial phenol in solution partitions to the fiber by the end of the experiment, which is considered negligible under the methodology of Endo et al.<sup>27</sup> One sample, eugenol with ammonium sulfate, exceeds our typical range with 5.5% depletion at the highest salt concentration, though the data is still very linear ( $R^2 = 0.997$ ), and the calculated  $K_S$  remains constant. The generated data for nearly all salt and phenol combinations are very linear ( $R^2 >$ 0.99) and reproducible (RSD < 10%). However, the observed degree of salting out is very small and inconsistent between replicates for ammonium nitrate. We report values of Ks for our phenols with this salt and note the higher experimental errors (highest RSD = 50% with GA). Wang et al. also observed significantly larger experimental errors when testing compounds for which the ammonium nitrate salt effect was very small: the values of some phenols tested (4fluorophenol and 4-iodophenol) were so small and scattered that the data were not reported.<sup>24</sup> As shown in Figure 4, the degree of salting out depends upon the salt identity, and the trend is consistent between compounds. Ranked from greatest to least, the order of  $K_S$  is  $(NH_4)_2SO_4 >$ NaCl > NH<sub>4</sub>Cl ≥ KNO<sub>3</sub> > NH<sub>4</sub>NO<sub>3</sub>, consistent with the findings of Wang et al.<sup>24</sup> For our six phenols, average  $K_S$  values for these salts are 0.49, 0.22, 0.12, 0.10, and 0.038  $M^{-1}$ , respectively (Table S5). For reference, K<sub>S</sub> values of 0.038 and 0.49 would reduce the aqueous concentrations in a 1 M salt solution by 8 and 33 percent, respectively. Our measurements are similar to those of Wang et al., who measured average Ks values for all tested compounds of 0.50, 0.24, 0.12, and 0.07 for (NH<sub>4</sub>)<sub>2</sub>SO<sub>4</sub>, NaCl, NH<sub>4</sub>Cl, and NH<sub>4</sub>NO<sub>3</sub>, respectively. <sup>24</sup> K<sub>S</sub> values for the four phenols analyzed by Wang et al. (bisphenol A, 2-phenylphenol, 4-fluorophenol, and 4-iodophenol) are 0.34, 0.20, 0.08, and 0.038, respectively. The similarity between our values and those of Wang et al. suggests that, for similar structure types (e.g., phenols), and perhaps even more broadly, the

264

265

266

267

268

269

270

271

272

273

274

275

276

277

278

279

280

281

282

283

284

impact of salt addition is relatively consistent, and may be applied to determine the approximate salt effect for other structures for which no  $K_S$  data exists.

*Implications* 

Air-water partitioning impacts the distribution of species, which affects their chemical fates and lifetimes. For example, phenols can be oxidized in both the gas phase and aqueous phase, which have different pathways, different products, and different yields of SOA.<sup>6-9, 36, 37</sup> An accurate measure of the aqueous fraction is therefore vital to understanding atmospheric processing in both phases, the rates of SOA formation, and the impacts of the SOA. The fraction of a species present in the aqueous phase (e.g., cloud drop or aerosol liquid water) is equal to:

$$f_{aq} = \frac{1}{1 + \frac{1}{K_H LRT}}$$
 (7)

where L is the liquid water content ( $L_{aq} L_{air}^{-1}$ ), R is the gas constant, and T is the temperature. Figure 5 shows calculated aqueous fractions at 278 K for typical cloud conditions ( $L = 10^{-7} L_{aq} L_{air}^{-1}$ , i.e., 0.1 g m<sup>-3</sup>) and a high liquid water content aerosol ( $10^{-10} L_{aq} L_{air}^{-1}$ , i.e., 100  $\mu$ g m<sup>-3</sup>) where the impact of salts is ignored. Based upon past measurements and our GA and Zing results (Table S5), we use an average  $\Delta H_{sol}$  value of -65.3 kJ mol<sup>-1</sup> to adjust our  $K_{H}$  values to colder temperatures when no measured data exists.

As shown in Figure 5, in cloud water the aqueous fractions of the lower- $K_H$  species such as guaiacol are around 1 percent (e.g., 1.2% for guaiacol). Under particle water conditions, the aqueous fraction for these compounds is much smaller, approximately 0.001%. In contrast, at the high end of our Henry's law scale, we calculate nearly complete ( $\geq 95\%$ ) aqueous partitioning for GA, Zing, VanOH, and SA as well as major aqueous partitioning for VanEth (70%) under

cloud conditions. Under dilute conditions (cloud and fog drops), we do not expect significant salting out. Salt concentrations in cloud and fog drops are typically less than 5 mM, which would cause less than a 1% decrease in aqueous partitioning using our measured  $K_S$  values.

For air-water partitioning under particle water conditions, as a first cut we ignore the impact of salt. At a liquid water content of  $10^{-10}$  L<sub>aq</sub> L<sub>air</sub>-1, SA is the only compound found primarily in the aqueous phase (65%). Under these conditions 13% of VanOH is predicted to partition into particle water, while even smaller aqueous fractions of Zing (3%), GA (2%), VanEth (0.2%) are predicted. Eug, Gua, and PropGua will essentially remain in the gas phase, with less than 0.001% in particle water at equilibrium.

We next consider the impact of salts on partitioning. Based on PM measurements and thermodynamic modeling, salt concentrations can span a wide concentration range, up to 30 M for salts like ammonium nitrate in areas with significant agricultural and urban emissions (e.g., California's Central Valley). <sup>38</sup> Figure 6 shows the effect of salt concentration on the Henry's law partitioning using the average Ks value across our eight phenols for each salt (Table S4). Compared to dilute solution, aqueous phenol concentrations are lower by a factor of 270 in 5 M ammonium sulfate and by a factor of 1.5 in 5 M ammonium nitrate (i.e.,  $C_{\text{salt}}/C_{\text{water}} = 0.0037$  and 0.65, respectively). Thus, we might expect far less salting out in wintertime Central Valley particles, where ammonium nitrate is dominant, relative to particles on the U.S. East Coast, where ammonium sulfate is more abundant.

While high concentrations of some salts can inhibit the partitioning of species to particle water, there is also evidence that partitioning of organics into drops and ALW might exceed predictions from Henry's law. For example, field measurements of methoxyphenols in fog waters reveal

aqueous concentrations up to 10-fold greater than predicted from  $K_{\rm H}$ .<sup>39</sup> Other studies observed similar fog enhancements in the aqueous partitioning of organophosphorus pesticides, <sup>40</sup> n-alkanes, and other organics, including phenol.<sup>41</sup>. One potential reason for this enhanced aqueous partitioning is the presence of dissolved organic matter (DOM).<sup>42-44</sup> DOM can decrease the surface tension of drop water, indicating some surface active components, <sup>41, 45, 46</sup> and these compounds may facilitate partitioning into the aqueous phase. Under ALW conditions, where we might expect elevated DOM concentrations (on the order of a few molar), this high organic content could enhance aqueous partitioning. Other particulate species released from biomass burning, such as cellulose-derived sugars (e.g., levoglucosan, galactose, mannosan) and ligninderived acids (e.g., veratric, vanillic) may also enhance partitioning of phenols and other semi-volatile organics into atmospheric water.

# 341 FIGURES

342

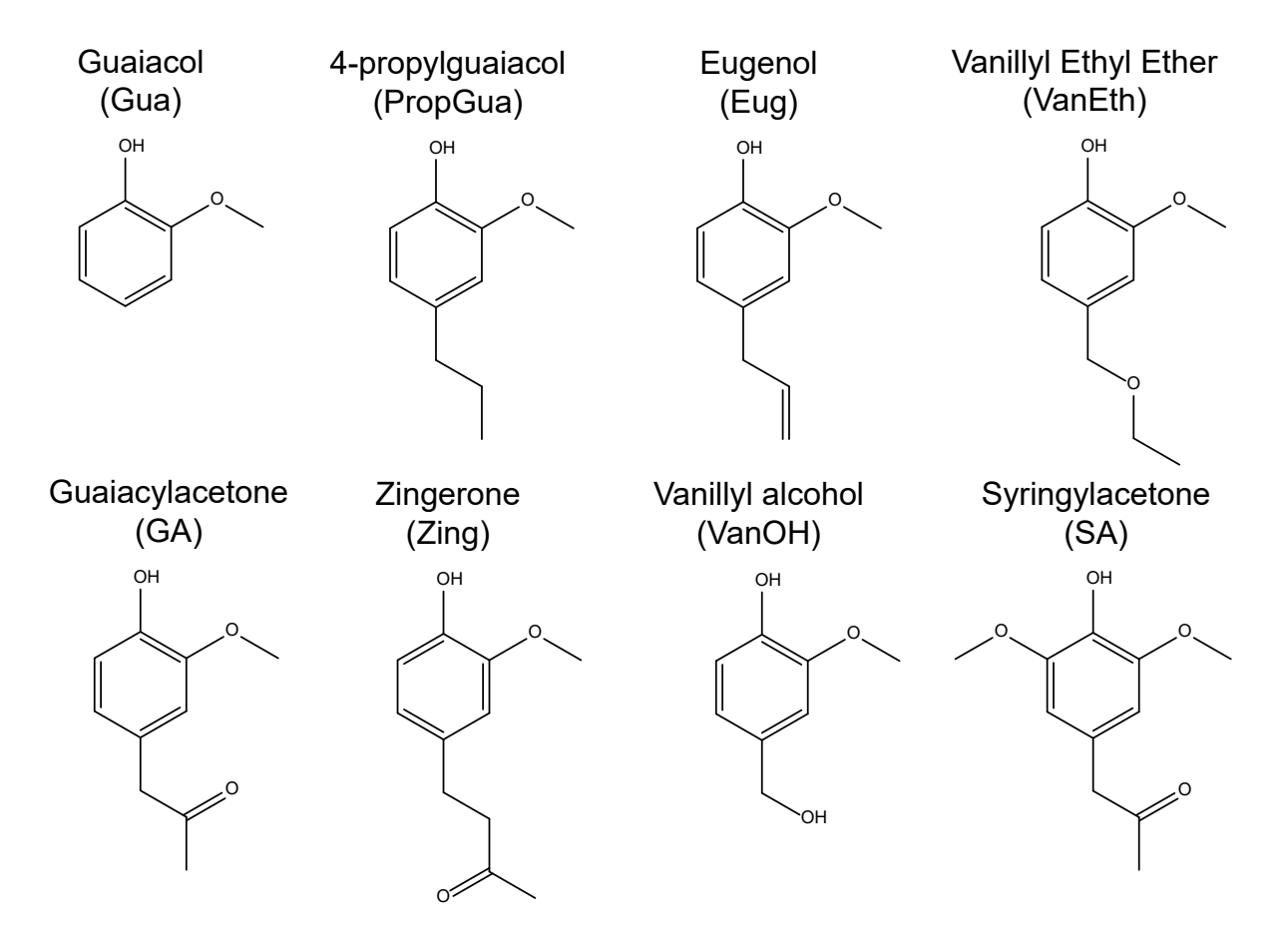
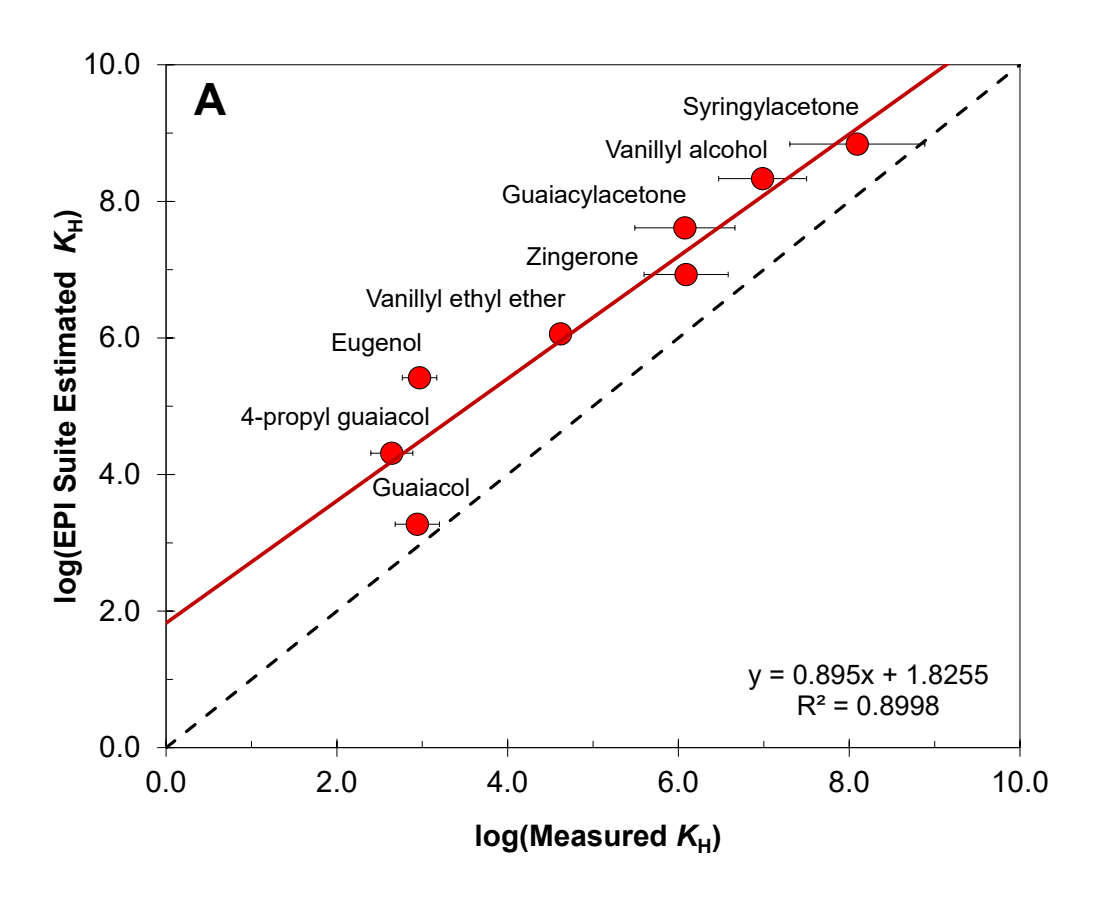
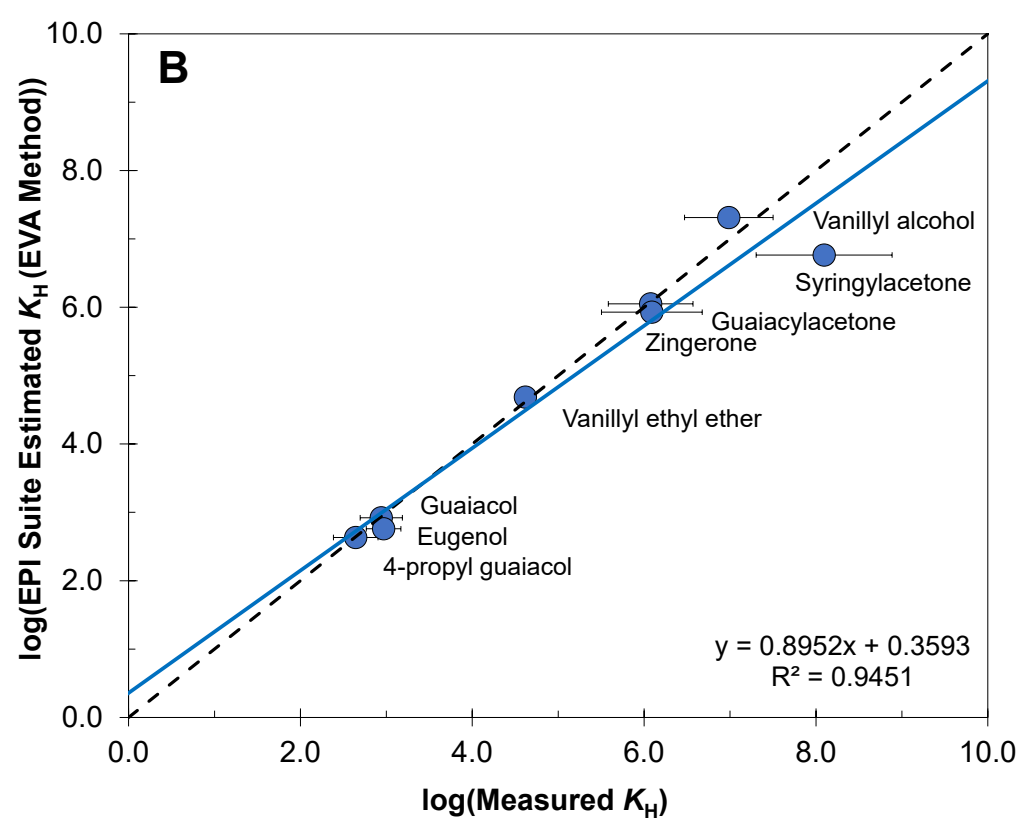
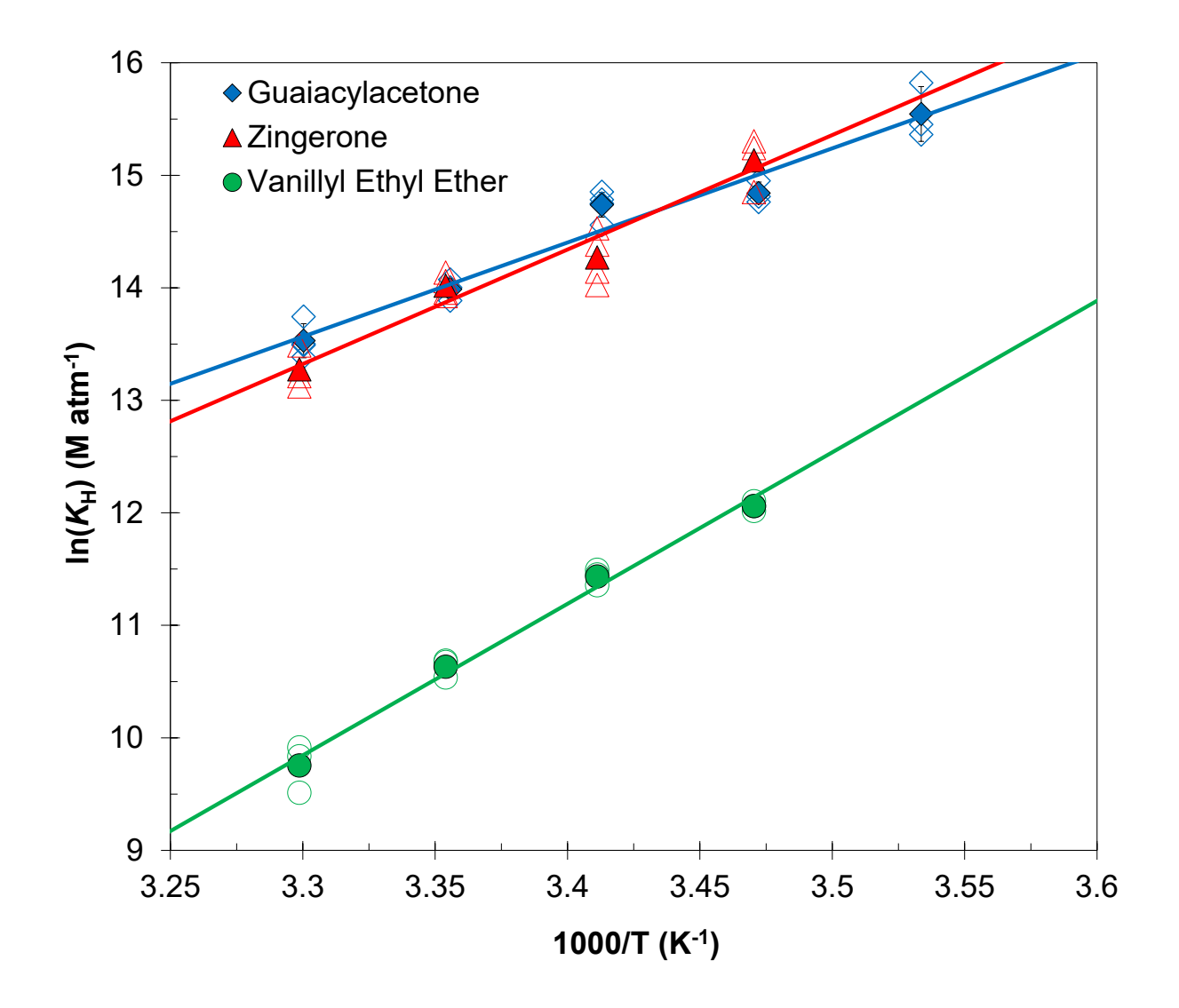


Figure 1. Structures, names, and abbreviations of the biomass-burning phenols included in this study.





**Figure 2.** Comparison of measured values (298 K) of  $K_H$  with predicted values from (A) EPI Suite bond method and (B) EPI Suite Experimental Value Adjustment (EVA) method. Guaiacol was used in the EVA calculation as the known  $K_H$  constant for 4-propylguaiacol, eugenol, vanillyl ethyl ether, zingerone, and guaiacylacetone. 4-methylguaiacol was used for vanillyl alcohol while syringol was used for syringylacetone. Error bars represent  $\pm 1\sigma$  for all compounds except SA, for which the standard error of a single experiment is represented. Data are summarized in Table S5. The dashed lines are 1:1 lines.



355

356

357

358

359

360

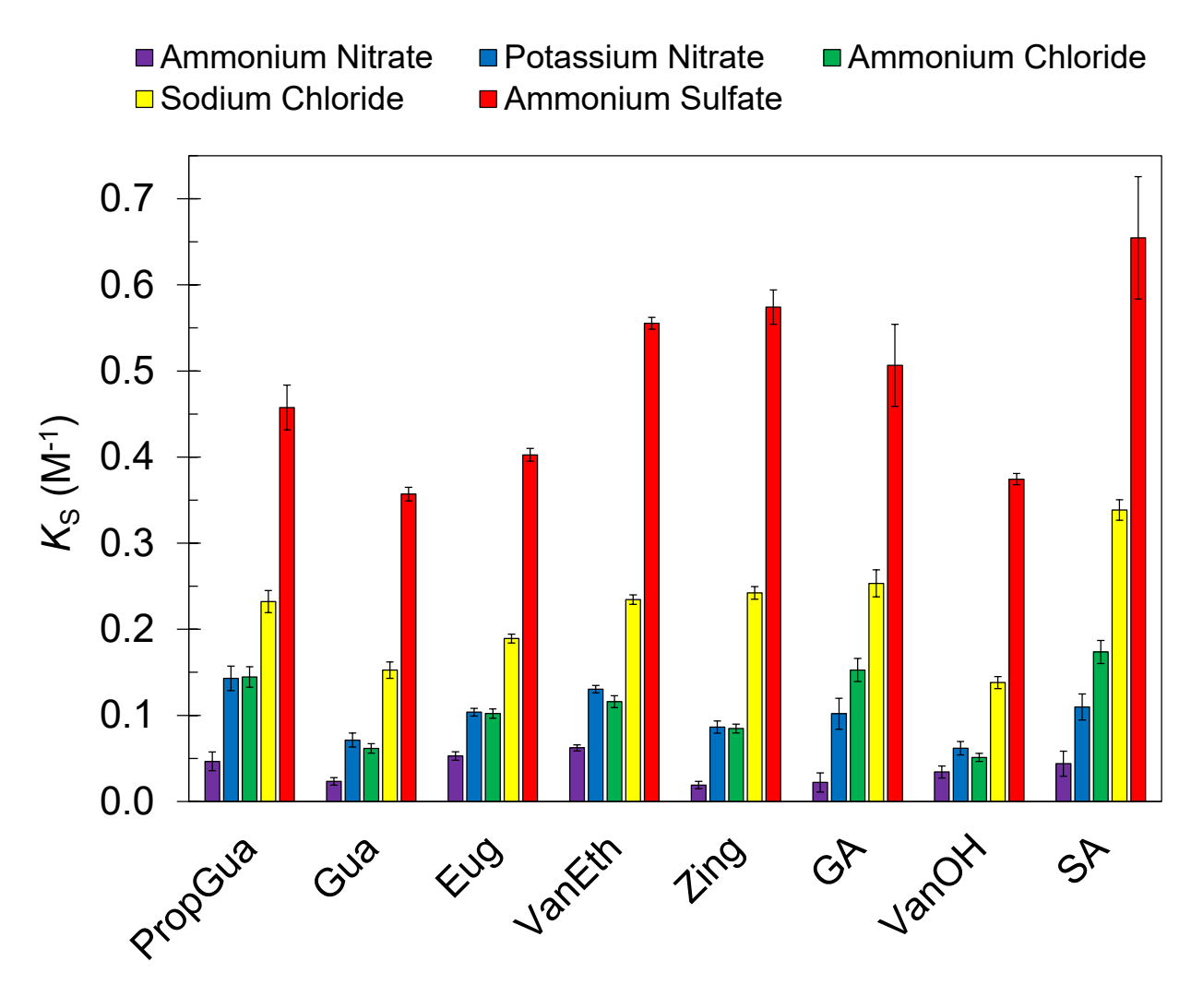


**Figure 4.** Summary of salting out data for phenols tested in this work. Error bars represent  $\pm 1\sigma$  of at least three measurements. Data are listed in Table S4.

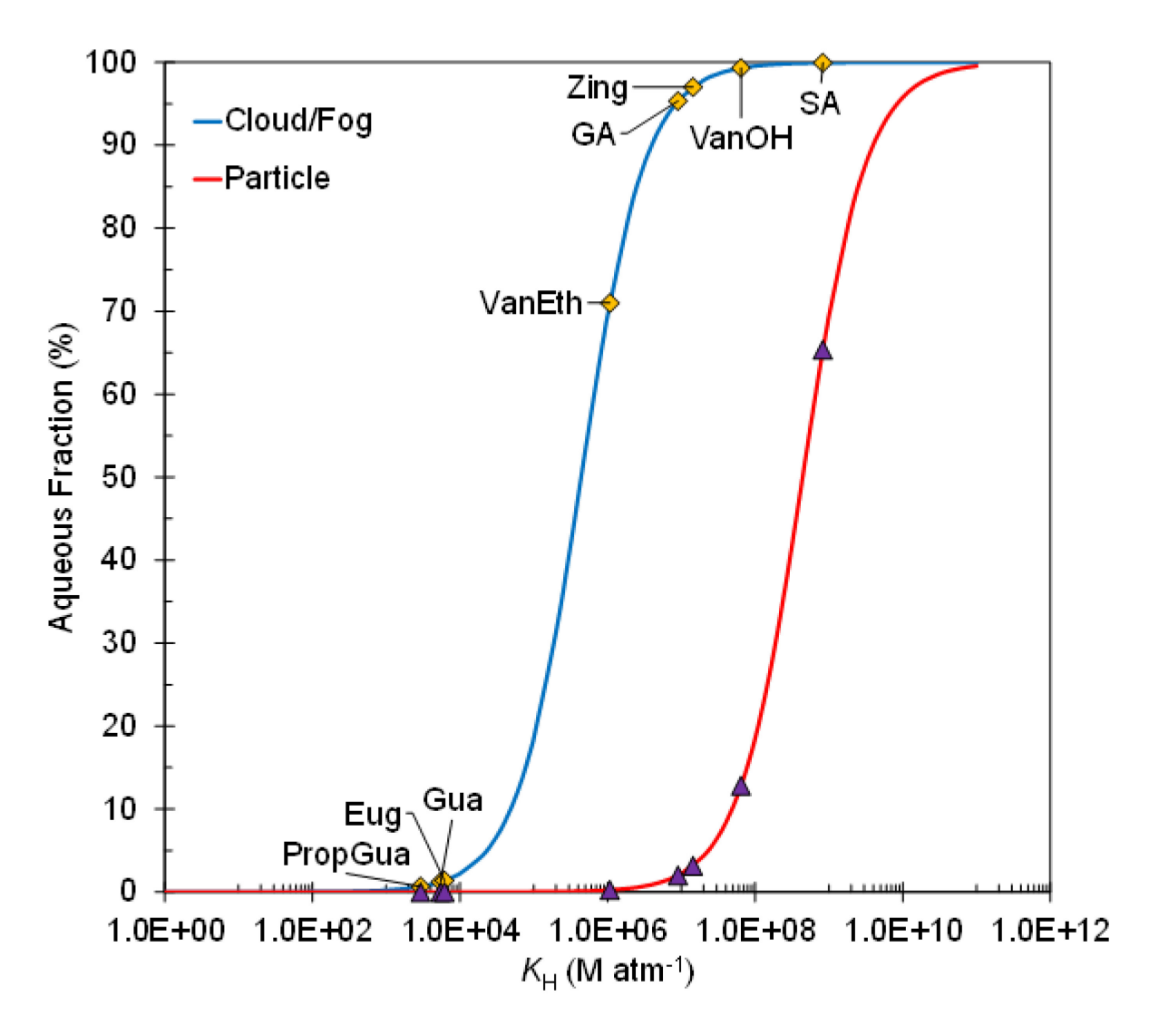


**Figure 5.** Aqueous fraction as a function of  $K_{\rm H}$  under cloud (0.1 g-H<sub>2</sub>O m<sup>-3</sup>) and particle (100 μg-H<sub>2</sub>O m<sup>-3</sup>) liquid water conditions at 278 K. The expected aqueous fraction of each phenol was calculated using our measured  $K_{\rm H}$  values adjusted to 278 K using measured values of  $\Delta H_{\rm sol}$  when available or, when not, the average of the measured phenol values, 65.3 kJ mol<sup>-1</sup>; with this enthalpy of solvation,  $K_{\rm H}$  increases by a factor of 6.3 to 26 at 278 K compared to 298 K. Aqueous fractions are shown as points for both cloud (yellow diamonds) and particle (purple triangles) water conditions.

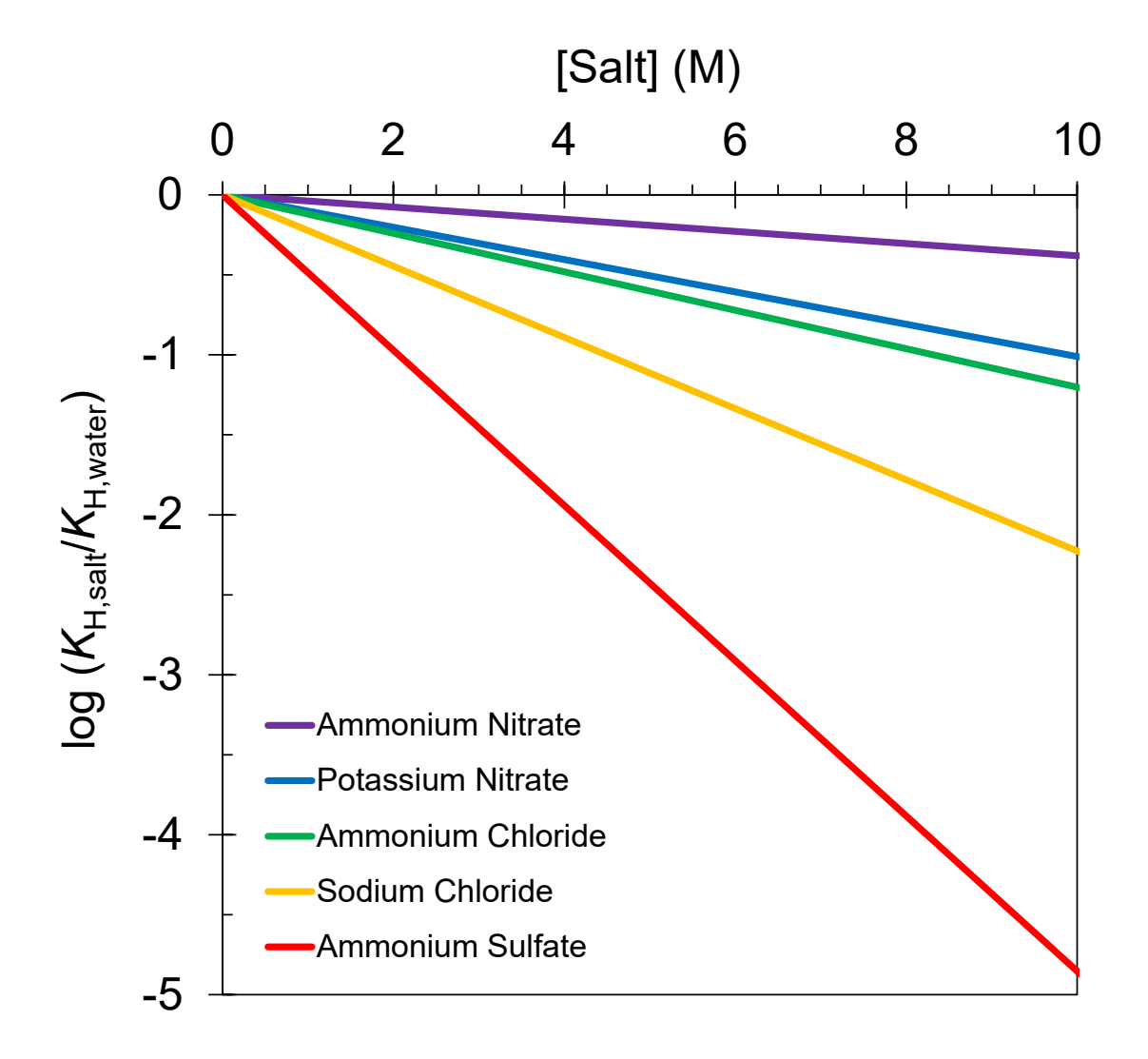


**Figure 6.** Effect of salt concentration on Henry's law partitioning. Lines are calculated using the average value of  $K_S$  across all phenols.

#### SUPPORTING INFORMATION

Description of system construction, flow rate setting, and validation (Section S1). Detailed schematic of system used (Figure S1). Effect of incomplete system conditioning on sample collection (Figure S2). Dependence of Henry's law constant on system flow rate (Figure S3). Examples of generated experimental data for  $K_H$  (Figure S4) and  $K_S$  (Figure S5). Temperature dependences for selected phenols (Figure S6). Relationship between  $K_H$  and  $\Delta H_{Sol}$  for measured and literature phenols (Figure S7). Detailed list of system components (Table S1). Percent recoveries from XAD resin for each phenol (Table S2). Details on mass spectrometer and chromatographic conditions for all compounds (Table S3a and S3b). Tabulated values of  $K_H$  (Table S4) and  $K_S$  (Table S5) for all tested compounds. Tabulated values of measured and EVA-predicted  $K_H$  values, along with  $\Delta H_{Sol}$  values for an extended suite of woodsmoke phenols (Table S6).

#### **AUTHOR INFORMATION**

# **Corresponding Author**

\*Cort Anastasio. Tel: 530-754-6095, Email: canastasio@ucdavis.edu

### **Author Contributions**

AM and AJ designed and carried out the experiments and analysis with input from CA. AM prepared this manuscript with input from CA. All authors have given approval to the final version of this manuscript.

#### **ACKNOWLEDGMENTS**

- We wish to thank Matt Hengel and Zachary Redman for their assistance with LC-MS materials,
- training, and troubleshooting. This research was funded by National Science Foundation grant
- 397 (AGS-1649212), and a Jastro Shields Research Award, Donald G. Crosby Fellowship and Victor
- 398 Chu Fellowship from UC Davis.

400

#### **ABBREVIATIONS**

- 401 Secondary organic aerosol (SOA), Henry's law constant  $(K_H)$ , Setschenow coefficient  $(K_S)$ ,
- 402 primary organic aerosol (POA), triplet excited states of carbon (<sup>3</sup>C\*), aqueous secondary organic
- aerosol (aqSOA), aerosol liquid water (ALW), quantitative structure activity relationships
- 404 (QSARs), experimental value adjustment (EVA), vanillyl alcohol (VanOH), vanillyl ethyl ether
- 405 (VanEth), 4-propylguaiacol (PropGua), zingerone (Zing), guaiacylacetone (GA), guaiacol (Gua),
- 406 eugenol (Eug), ethylenediaminetetraacetic acid (EDTA), syringylacetone (SA), solid phase micro
- 407 extraction (SPME), dissolved organic matter (DOM).

#### 408 **REFERENCES**

- 409 1. Bond, T. C.; Doherty, S. J.; Fahey, D.; Forster, P.; Berntsen, T.; DeAngelo, B.; Flanner, M.;
- Ghan, S.; Kärcher, B.; Koch, D., Bounding the role of black carbon in the climate system: A
- scientific assessment. *Journal of Geophysical Research: Atmospheres* **2013**, *118*, (11), 5380-5552.
- 2. Randerson, J. T.; Liu, H.; Flanner, M. G.; Chambers, S. D.; Jin, Y.; Hess, P. G.; Pfister, G.;
- Mack, M. C.; Treseder, K. K.; Welp, L. R.; Chapin, F. S.; Harden, J. W.; Goulden, M. L.;
- Lyons, E.; Neff, J. C.; Schuur, E. A. G.; Zender, C. S., The Impact of Boreal Forest Fire on Climate Warming. *Science* **2006**, *314*, (5802), 1130.
- 3. Reisen, F.; Duran, S. M.; Flannigan, M.; Elliott, C.; Rideout, K., Wildfire smoke and public health risk. *International Journal of Wildland Fire* **2015**, *24*, (8), 1029-1044.
- 419 4. Monks, P. S.; Granier, C.; Fuzzi, S.; Stohl, A.; Williams, M. L.; Akimoto, H.; Amann, M.;
- Baklanov, A.; Baltensperger, U.; Bey, I.; Blake, N.; Blake, R. S.; Carslaw, K.; Cooper, O. R.;
- Dentener, F.; Fowler, D.; Fragkou, E.; Frost, G. J.; Generoso, S.; Ginoux, P.; Grewe, V.;
- Guenther, A.; Hansson, H. C.; Henne, S.; Hjorth, J.; Hofzumahaus, A.; Huntrieser, H.;
- Isaksen, I. S. A.; Jenkin, M. E.; Kaiser, J.; Kanakidou, M.; Klimont, Z.; Kulmala, M.; Laj, P.;
- Lawrence, M. G.; Lee, J. D.; Liousse, C.; Maione, M.; McFiggans, G.; Metzger, A.; Mieville,
- 425 A.; Moussiopoulos, N.; Orlando, J. J.; O'Dowd, C. D.; Palmer, P. I.; Parrish, D. D.; Petzold,

- 426 A.; Platt, U.; Pöschl, U.; Prévôt, A. S. H.; Reeves, C. E.; Reimann, S.; Rudich, Y.; Sellegri,
- 427 K.; Steinbrecher, R.; Simpson, D.; ten Brink, H.; Theloke, J.; van der Werf, G. R.; Vautard,
- R.; Vestreng, V.; Vlachokostas, C.; von Glasow, R., Atmospheric composition change global and regional air quality. *Atmospheric Environment* **2009**, *43*, (33), 5268-5350.
- 5. Schauer, J. J.; Kleeman, M. J.; Cass, G. R.; Simoneit, B. R. T., Measurement of Emissions from Air Pollution Sources. 3. C1–C29 Organic Compounds from Fireplace Combustion of
- 432 Wood. *Environmental Science & Technology* **2001,** *35*, (9), 1716-1728.
- 6. Smith, J. D.; Sio, V.; Yu, L.; Zhang, Q.; Anastasio, C., Secondary Organic Aerosol Production from Aqueous Reactions of Atmospheric Phenols with an Organic Triplet Excited State.
- 435 Environmental Science & Technology **2014**, 48, (2), 1049-1057.
- 7. Smith, J. D.; Kinney, H.; Anastasio, C., Aqueous benzene-diols react with an organic triplet excited state and hydroxyl radical to form secondary organic aerosol. *Physical Chemistry Chemical Physics* **2015**, *17*, (15), 10227-10237.
- 8. Smith, J. D.; Kinney, H.; Anastasio, C., Phenolic carbonyls undergo rapid aqueous photodegradation to form low-volatility, light-absorbing products. *Atmospheric Environment* **2016**, *126*, 36-44.
- Yu, L.; Smith, J.; Laskin, A.; George, K. M.; Anastasio, C.; Laskin, J.; Dillner, A. M.; Zhang,
   Q., Molecular transformations of phenolic SOA during photochemical aging in the aqueous
   phase: competition among oligomerization, functionalization, and fragmentation. *Atmos. Chem. Phys.* 2016, 16, (7), 4511-4527.
- 446 10. Ervens, B.; Turpin, B.; Weber, R., Secondary organic aerosol formation in cloud droplets and aqueous particles (aqSOA): a review of laboratory, field and model studies. *Atmospheric Chemistry and Physics* **2011**, *11*, (21), 11069-11102.
- 11. Sander, R., Compilation of Henry's law constants (version 4.0) for water as solvent. *Atmos. Chem. Phys.* **2015,** *15*, (8), 4399-4981.
- 451 12. Herrmann, H.; Schaefer, T.; Tilgner, A.; Styler, S. A.; Weller, C.; Teich, M.; Otto, T.,
  452 Tropospheric Aqueous-Phase Chemistry: Kinetics, Mechanisms, and Its Coupling to a
  453 Changing Gas Phase. *Chemical Reviews* **2015**, *115*, (10), 4259-4334.
- 13. EPA, U. S. *Estimation Programs Interface Suite* TM for Microsoft® Windows, v 4.11; United States Environmental Protection Agency: Washington, DC, USA, 2012.
- 456 14. Meylan, W. M.; Howard, P. H., Bond contribution method for estimating Henry's law constants. *Environmental toxicology and chemistry* **1991**, *10*, (10), 1283-1293.
- 458 15. Hine, J.; Mookerjee, P., Intrinsic Hydrophilic Character of Organic Compounds: Correlations in Terms of Structural Contributions. *Journal of Organic Chemistry* **1975**, *40*, (3).
- 460 16. Card, M. L.; Gomez-Alvarez, V.; Lee, W.-H.; Lynch, D. G.; Orentas, N. S.; Lee, M. T.; Wong, E. M.; Boethling, R. S., History of EPI Suite<sup>TM</sup> and future perspectives on chemical property estimation in US Toxic Substances Control Act new chemical risk assessments. *Environmental Science: Processes & Impacts* **2017**, *19*, (3), 203-212.
- Tolocka, M. P.; Lake, D. A.; Johnston, M. V.; Wexler, A. S., Size-resolved fine and ultrafine particle composition in Baltimore, Maryland. *Journal of Geophysical Research: Atmospheres* 2005, 110, (D7).
- 18. Finlayson-Pitts, B. J.; Pitts Jr, J. N., *Chemistry of the Upper and Lower Atmosphere: Theory, Experiments, and Applications.* Academic press: 1999.
- 19. Seinfeld, J. H.; Pandis, S. N., Atmospheric Chemistry and Physics From Air Pollution to Climate Change. In 2 ed.; Wiley: Hoboken, N.J., 2006.

- 471 20. Setschenow, J., Über die Konstitution der Salzlösungen auf Grund ihres Verhaltens zu Kohlensäure. In *Zeitschrift für Physikalische Chemie*, 1889; Vol. 4U, p 117.
- 21. Schwarzenbach, R. P.; Gschwend, P. M.; Imboden, D. M., Organic liquid–water partitioning. **2003**.
- 22. Zhou, W.; Mekic, M.; Liu, J.; Loisel, G.; Jin, B.; Vione, D.; Gligorovski, S., Ionic strength effects on the photochemical degradation of acetosyringone in atmospheric deliquescent aerosol particles. *Atmospheric Environment* **2019**, *198*, 83-88.
- 478 23. Mekic, M.; Brigante, M.; Vione, D.; Gligorovski, S., Exploring the ionic strength effects on the photochemical degradation of pyruvic acid in atmospheric deliquescent aerosol particles.

  480 Atmospheric Environment 2018, 185, 237-242.
- 481 24. Wang, C.; Lei, Y. D.; Wania, F., Effect of Sodium Sulfate, Ammonium Chloride, Ammonium 482 Nitrate, and Salt Mixtures on Aqueous Phase Partitioning of Organic Compounds.

  483 Environmental Science & Technology 2016, 50, (23), 12742-12749.
- Waxman, E. M.; Elm, J.; Kurten, T.; Mikkelsen, K. V.; Ziemann, P. J.; Vokamer, R., Glyoxal
   and Methylglyoxal Setschenow Salting Constants in Sulfate, Nitrate, and Chloride Solutions:
   Measurements and Gibbs Energies. *Environmental Science & Technology* 2015, 49, (19),
   11500-11508.
- 488 26. Fendinger, N. J.; Glotfelty, D. E., A laboratory method for the experimental determination of air-water Henry's law constants for several pesticides. *Environmental science & technology* 490 **1988**, *22*, (11), 1289-1293.
- 491 27. Endo, S.; Pfennigsdorff, A.; Goss, K.-U., Salting-Out Effect in Aqueous NaCl Solutions: Trends with Size and Polarity of Solute Molecules. *Environmental Science & Technology* **2012**, *46*, (3), 1496-1503.
- 28. Sagebiel, J. C.; Seiber, J. N.; Woodrow, J. E., Comparison of headspace and gas-stripping methods for determining the Henry's law constant (H) for organic compounds of low to intermediate H. *Chemosphere* **1992**, *25*, (12), 1763-1768.
- 497 29. Čenský, M.; Šedlbauer, J.; Majer, V.; Růžička, V., Standard partial molal properties of aqueous alkylphenols and alkylanilines over a wide range of temperatures and pressures.
  499 *Geochimica et Cosmochimica Acta* **2007**, *71*, (3), 580-603.
- 500 30. Feigenbrugel, V.; Le Calvé, S.; Mirabel, P.; Louis, F., Henry's law constant measurements for phenol, o-, m-, and p-cresol as a function of temperature. *Atmospheric Environment* **2004**, *38*, 502 (33), 5577-5588.
- 503 31. Sheikheldin, S. Y.; Cardwell, T. J.; Cattrall, R. W.; Luque de Castro, M. D.; Kolev, S. D.,
  504 Determination of Henry's Law Constants of Phenols by Pervaporation-Flow Injection
  505 Analysis. *Environmental Science & Technology* **2001**, *35*, (1), 178-181.
- 506 32. Harrison, M. A. J.; Cape, J. N.; Heal, M. R., Experimentally determined Henry's Law coefficients of phenol, 2-methylphenol and 2-nitrophenol in the temperature range 281–302K.

  Atmospheric Environment 2002, 36, (11), 1843-1851.
- 509 33. Dohnal, V.; Fenclova, D., Air-water partitioning and aqueous solubility of phenols. *Journal* of Chemical and Engineering Data 1995, 40, (2), 478-483.
- 34. Mackay, D.; Shiu, W.-Y.; Lee, S. C., *Handbook of physical-chemical properties and environmental fate for organic chemicals.* CRC press: 2006.
- 513 35. Toivola, M.; Prisle, N. L.; Elm, J.; Waxman, E. M.; Volkamer, R.; Kurtén, T., Can 514 COSMOTherm predict a salting in effect? *The Journal of Physical Chemistry A* **2017**, *121*, 515 (33), 6288-6295.

- 36. Eddingsaas, N.; Loza, C.; Yee, L.; Chan, M.; Schilling, K.; Chhabra, P.; Seinfeld, J.;
   Wennberg, P., α-pinene photooxidation under controlled chemical conditions—Part 2: SOA yield and composition in low-and high-NO\_x environments. *Atmospheric Chemistry and Physics* 2012, 12, (16), 7413-7427.
- 520 37. Eddingsaas, N.; Loza, C.; Yee, L.; Seinfeld, J.; Wennberg, P., α-pinene photooxidation under controlled chemical conditions—Part 1: Gas-phase composition in low-and high-NO x environments. *Atmospheric Chemistry and Physics* **2012**, *12*, (14), 6489-6504.
- 523 38. Parworth, C. L.; Young, D. E.; Kim, H.; Zhang, X.; Cappa, C. D.; Collier, S.; Zhang, Q., Wintertime water-soluble aerosol composition and particle water content in Fresno, California. *Journal of Geophysical Research: Atmospheres* **2017**, *122*, (5), 3155-3170.
- 39. Sagebiel, J. C.; Seiber, J. N., Studies on the occurrence and distribution of wood smoke marker compounds in foggy atmospheres. *Environmental Toxicology and Chemistry: An International Journal* **1993**, *12*, (5), 813-822.
- 529 40. Glotfelty, D. E.; Majewski, M. S.; Seiber, J. N., Distribution of several organophosphorus 530 insecticides and their oxygen analogs in a foggy atmosphere. *Environmental Science & Technology* **1990**, *24*, (3), 353-357.
- 532 41. Capel, P. D.; Leuenberger, C.; Giger, W., Hydrophobic organic chemicals in urban fog. 533 Atmospheric Environment. Part A. General Topics 1991, 25, (7), 1335-1346.
- 534 42. Donaldson, D. J.; Vaida, V., The Influence of Organic Films at the Air-Aqueous Boundary on Atmospheric Processes. *Chemical Reviews* **2006**, *106*, (4), 1445-1461.
- 536 43. Tervahattu, H.; Hartonen, K.; Kerminen, V. M.; Kupiainen, K.; Aarnio, P.; Koskentalo, T.; 537 Tuck, A. F.; Vaida, V., New evidence of an organic layer on marine aerosols. *Journal of Geophysical Research: Atmospheres* **2002**, *107*, (D7), AAC 1-1-AAC 1-8.
- 539 44. Russell, L. M.; Maria, S. F.; Myneni, S. C., Mapping organic coatings on atmospheric particles. *Geophysical Research Letters* **2002**, *29*, (16), 26-1-26-4.
- Liang, C.; Pankow, J. F.; Odum, J. R.; Seinfeld, J. H., Gas/particle partitioning of semivolatile
   organic compounds to model inorganic, organic, and ambient smog aerosols. *Environmental Science & Technology* 1997, 31, (11), 3086-3092.
- 544 46. Goss, K.-U., The air/surface adsorption equilibrium of organic compounds under ambient 545 conditions. *Critical Reviews in Environmental Science and Technology* **2004**, *34*, (4), 339-546 389.

1	Supporting Information for			
2	Air-Water Partitioning of Biomass Burning Phenols			
3	and the Effects of Temperature and Salinity			
4	Alexander S. McFall, Alex W. Johnson, and Cort Anastasio			
5	University of California, Davis			
6	1 Shields Avenue, Davis, CA 95616			
7	Submitted to Environmental Science and Technology: 25 October 2019			
8	Revised Version Submitted: 13 January 2020			
9				
10	This Supporting Information contains 20 pages (S1 to S20):			
11 12	Section S1 describes the system used for Henry's law measurement and its validation using guaiacol.			
13	Figure S1 presents a detailed schematic of the system used.			
14	Figure S2 presents the effect of incomplete system conditioning on sample collection.			
15	Figure S3 presents the dependence of guaiacol Henry's law constant on system flow rate.			
16	Figure S4 presents an example of generated $K_{\rm H}$ data for vanillyl ethyl ether.			
17	Figure S5 presents measured $K_S$ data for guaiacol.			
18	Figure S6 displays experimentally determined temperature dependences for selected phenols			
19	in van't Hoff form.			
20	Figure S7 gives the relationship between $K_{\rm H}$ and $\Delta H_{\rm sol}$ for measured and literature phenols.			
21 22	Table S1 presents a detailed list of system components.			
23	Table S2 tabulates the percent recoveries of each phenol from XAD-4 resin extraction. Table S3a summarizes the mass spectrometer and chromatographic conditions used for $K_H$			
24	experiments.			
25	Table S3b summarizes the time segments and chromatographic conditions used for $K_S$			
26	experiments containing more than one phenol.			
27	Table S4 tabulates the measured Henry's law constants ( $K_{\rm H}$ ) for all tested phenols.			
28	Table S5 tabulates the measured Setschenow coefficients (Ks) for all tested phenols.			
29	Table S6 tabulates the $K_{\rm H}$ and $\Delta H_{\rm sol}$ values for a suite of additional woodsmoke phenols.			

# S1. Equilibrium Partitioning System Design and Validation

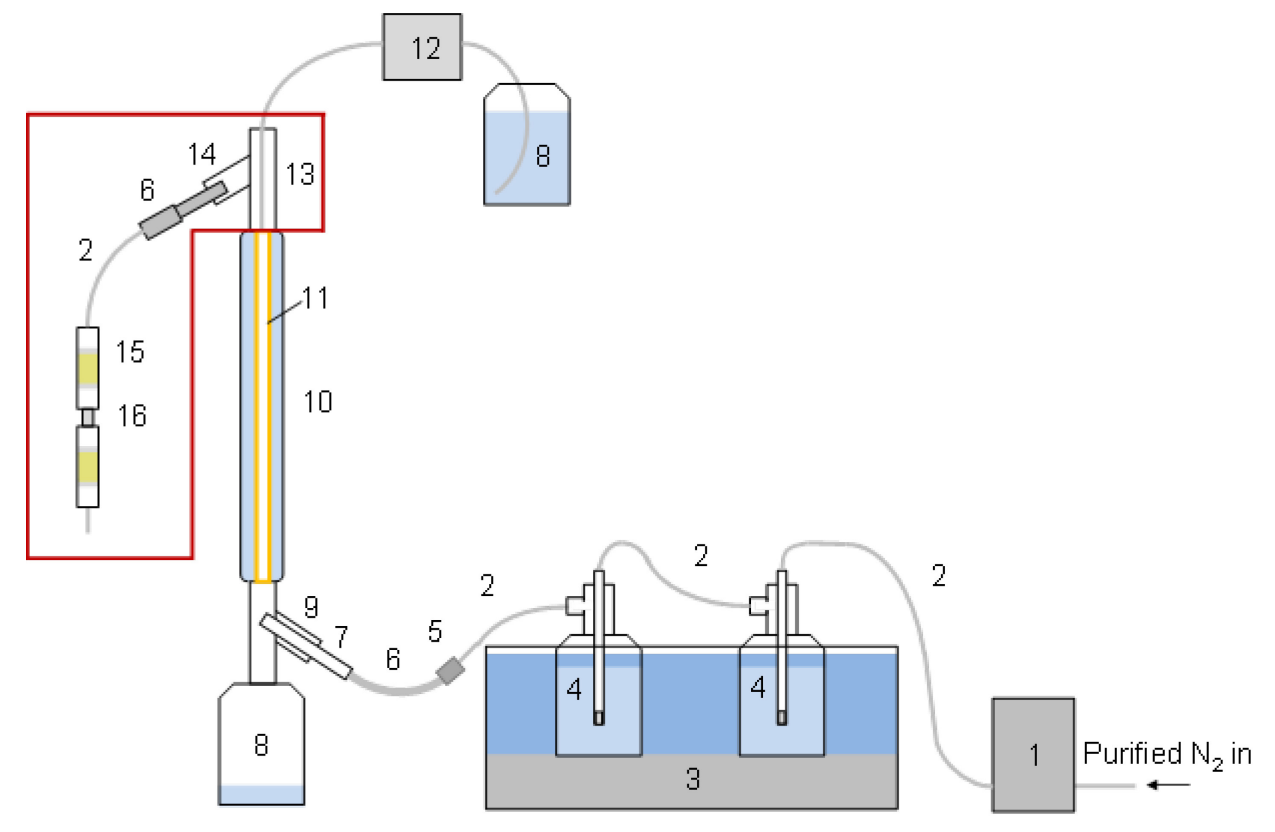


**Figure S1.** Schematic of the system for Henry's law determination. Purified, humidified nitrogen enters a wetted-wall column lined with glass fiber filter to saturate the gas flow with the compound of interest. The gas flow is then collected on XAD-4 resin for extraction and analysis. The area enclosed in red is wrapped with two thermostatic heating tapes maintained slightly above the experimental temperature to prevent water condensation. Numbers correspond to components listed in Table S1.

# **Table S1. System Materials**

Number	Manufacturer	Part Number	Description and Notes
1	MKS Instruments	1179A	Mass Flow Controller
2	N/A	N/A	Teflon (PTFE) Tubing, 0.25 in OD, 0.125 in ID
3	NESLAB	RTE-211	Refrigerated Bath/Circulator
4	Ace Glass	7532-06	Midget bubbler (top only) in 500 mL glass bottle (#8) with 24/40 ground glass joint
5	McMaster-Carr	4464K213 5361K41	304 Stainless Steel Threaded Pipe Fitting Medium-Pressure, Straight Connector, 3/8 NPT Female; 304 Stainless Steel Barbed Hose Fitting 1/2" Hose ID, 3/8 NPT Male End; 304 Stainless Steel Barbed Hose Fitting 1/4" Hose ID, 3/8 NPT Male End
6	N/A	N/A	Teflon (PTFE) Tubing, 0.5 in OD, 0.375 in ID
7	Ace Glass	13290-34	Adapter, maxi, AceThred, 24/40 outer to #15 AceThred
8	Ace Glass	5345-12	24/40 500 mL bottle. The top reservoir contains the phenol solution, while the bottom reservoir collects the waste.
9	Ace Glass	5045-10	Side arm adapter, 75 degree, 24/40 outer joints top and side, 24/40 inner joint bottom
10	Ace Glass	5998-17	Condenser, Liebig, 600 mm jacketed length, 24/40
11	Pall Corp.	61638	Type A/E Glass Fiber Sheets, 1 μm pore, 8 x 10 in.
12	WPI	504011	Ministar peristaltic pump with 2.4 mm ID silicone peristaltic tubing.
13	Ace Glass	5092-54	Side arm adapter, 75 degree with #7 AceThred on top, 24/40 inner joint side and bottom
14	Ace Glass	5030-40	Adapter, maxi, AceThred, 24/40 inner to #15 AceThred
7, 13, 14	Ace Glass	11710-03/15	Ferrules, PTFE, for use with #7 (-03) and #15 (-15) AceThred
15	Ace Glass	8700-50	10.058mm ID TruBore precision glass tubing, 61 cm length, approximately 12.5 mm OD
16	N/A	N/A	Bulkhead fittings, Teflon, 0.5 in. ID

A schematic of our system is shown above in Figure S1. Briefly, it consists of gas flow preparation, followed by gas-aqueous equilibrium partitioning in a wetted wall column, and finally sample gas collection. A detailed list of all system components is given in Table S1 for ease of reproduction. First, ultra-pure, dry nitrogen (Praxair, 99.999%) passes through an activated carbon filter (Whatman Carbon-Cap) and a 47 mm Teflon filter (Pall Corp., Teflo 3.0 µm pore) to remove particles before passing through a mass flow controller (1, MKS Instruments, Model 1179A). The N2 flows into a water bath set to the experimental temperature (3) that contains two sequential gas bubblers for humidification (4). This ensures that water doesn't evaporate from the reservoir solution as it flows through the column where gas-aqueous equilibrium is established.

The humidified gas then enters the wetted wall column (10), a 600-mm water-jacketed Liebig condenser lined with glass fiber filter (11, Pall Corp., Type A/E). Prior to use, we clean the filters with Milli-Q water (24-hour soak, 2 cycles), 1 M nitric acid (2-hour soak), and a final Milli-Q rinse to remove water soluble contaminants and metals, then bake them to dryness for 24 hours at 373 K. Without this cleaning, the reservoir solution increases from approximately pH 6 to near 9 within 30 minutes, and our tested phenols degrade rapidly. In tests using uncleaned filters with guaiacol and syringol, we observed 15 percent loss of both phenols after 30 minutes of filter contact, and a pH increase of over 3 units. Since the solution pH increases to near the pKa of our phenols, we suspect the degradation is due to formation of reactive phenolate ions. In contrast, using cleaned filters we observe neither significant phenol degradation nor an increase in pH. Above the condenser is a glass reservoir (8) containing an aqueous solution of the compound of interest (at a known concentration), which is supplied to the filter with a peristaltic pump (12, World Precision Instruments, Ministar) at a rate of 3 mL min<sup>-1</sup>. A thermometer inserted into the system through the top (where solution is delivered during an experiment) confirmed that, across the range of experimental temperatures (283 – 303 K), the exiting gas flow is within 0.5 K of the water bath temperature.

To ensure partitioning equilibrium in the column, we first calculated the maximum flow rate that enables sufficient residence time for diffusion to move the compound from the aqueous column walls into the gas flow.

We begin with the gaseous diffusion coefficient (also called diffusivity) for trace gases in air, estimated by:

$$D_G = 0.2 \left(\frac{T}{298}\right)^{1.75} \left(\frac{29}{\mu}\right)^{0.5}$$
 (S1)

- 73 where  $D_G$  is the gas-phase diffusion coefficient (cm<sup>2</sup> s<sup>-1</sup>), T is temperature (K), and  $\mu$  is the
- 74 molecular weight (g mol<sup>-1</sup>) of the compound of interest <sup>1</sup>. For guaiacol and guaiacylacetone, we
- 75 calculate gaseous diffusion coefficients of D = 0.0967 cm<sup>2</sup>/sec and D = 0.0802 cm<sup>2</sup>/sec,
- 76 respectively.
- 77 The residence time, t (min), of a molecule in our column is:

$$78 t = \frac{V}{Q} (S2)$$

- where  $V = \pi r^2 h$  is the column volume (cm<sup>3</sup>) and Q is the flow rate (cm<sup>3</sup> min<sup>-1</sup>).
- We consider diffusion in only one dimension, from the wall of the column into the gas
- stream. Given this condition, the diffusion distance, x, which a molecule can travel in time t is  $^2$ :

$$x^2 = 2Dt (S3)$$

Combining this with our residence time, we obtain:

$$x^2 = \frac{2D\pi r^2 h}{Q} \quad (S4)$$

- 65 Given our column length of 60 cm, we can rearrange Eq. S4 to solve for the maximum
- 86 flow rate where there is sufficient time for diffusion to reach gas-aqueous equilibrium in the
- 87 column:

$$Q = \frac{2D\pi r^2 h}{x^2} \quad (S5)$$

- If we assume that equilibrium is achieved when the phenol molecules in the solution on
- 90 the glass fiber filter only need to diffuse to the center of the inner tube, then this is equivalent to
- 91 assuming a diffusion distance of x = r. Under this condition equation S4 simplifies to:

$$Q = 2D\pi h \qquad (S6)$$

94

95

97

98

99

100

101

102

103

104

105

106

107

108

109

110

111

112

113

114

115

116

117

118

In the more stringent case where we assume that equilibrium is reached when the phenol molecules have sufficient time to diffuse from one side of the inner tube to the other, this is equivalent to x = 2r. Under this condition, equation S4 simplifies to

$$Q = \frac{D\pi h}{2} \quad (S7)$$

For this more stringent case, and our column height of h = 60 cm, we calculate maximum flow rates (O) of 454 and 547 cm<sup>3</sup> min<sup>-1</sup> for guaiacylacetone and guaiacol, respectively. Under the less stringent x = r assumption, flow rates are 2.19 and 1.81 L min<sup>-1</sup> for guaiacol and guaiacylacetone, respectively. For GA, we should be able to achieve equilibrium with flow rates up to 450 mL min<sup>-1</sup> under the most stringent diffusion assumptions. We use a gas flow of 50 mL min<sup>-1</sup> for guaiacol testing and 200 mL min<sup>-1</sup> for GA testing; these flow rates strike a balance between keeping experiment times short and depositing enough phenol on the XAD resin to readily quantify. After setting the reservoir and gas flows, we allow both to run without attaching the XAD-4 sample collector (8) in order to condition the system prior to sample collection. This ensures that any surfaces within the system that might adsorb the compound of interest have already done so prior to sample collection. The amount of conditioning time required is compound dependent, from approximately 1 hour for lower K<sub>H</sub> compounds (e.g. GUA, predicted vapor pressure 0.113 mm Hg, saturation concentration 7.6 x 10<sup>5</sup> µg m<sup>-3</sup> at 298 K) to overnight (ca. 12 hours) for higher  $K_{\rm H}$  compounds (e.g. GA, predicted vapor pressure 2.3 x  $10^{-4}$  mm Hg, saturation concentration 2.2 x 10<sup>3</sup> µg m<sup>-3</sup> at 298 K). With proper conditioning, a plot of the number of moles of gas-phase compound collected versus system run time is linear. In contrast, if the system is not fully conditioned the initial samples will be lower than expected because some of the gas-phase material is lost to the system inner walls, leading to a curved plot of gasphase amount versus time (Figure S2). A simple test for this is to run collections in reverse order, with the longest collection times first. Without full conditioning, the longest time point will be significantly lower than the line defined by the shorter time samples. After conditioning is achieved in the longest timepoint, the data will exhibit linear behavior for subsequent samples.

After the system is conditioned, the XAD-4 collection tube is connected to the 105-degree side-arm adapter to trap the compound of interest from the gas flow. The entire apparatus above the aqueous, jacketed column is wrapped with two programmable heating tapes (red outline, BriskHeat Model SDC120JC-A) and maintained at several degrees warmer than the aqueous column to ensure no condensation of water vapor in the glassware or Teflon. The top glassware was always maintained at 5 K warmer than the experimental temperature and the XAD plugs were held 2 K warmer.

119

120

121

122

123

124

125

126

127

128

129

130

131

132

133

134

135

136

137

138

139

140

141

142

143

144

145

146

147

148

XAD-4 resin is thoroughly cleaned prior to use. Batches of 1 L (dry volume) of XAD-4 are first stirred with 15 consecutive washes with 5 L of Milli-Q water to remove fines and watersoluble contaminants. After washing, the resin is soaked in Milli-Q water for 24 hours. The water is decanted off and the resin is transferred to an amber 4-liter bottle with 2 L of methanol and shaken for 24 hours on a shake table. This solvent shaking process is repeated with acetonitrile, and once again with methanol, with the solvent decanted into waste at each step. After solvent cleaning, the resin is transferred to a vacuum oven to dry overnight under mild vacuum at approximately 303 K. The prepared resin flows freely and shows no background contamination in replicate resin blank extractions. The resin is stored in sealed amber jars to prevent moisture and contaminant uptake from the air. For gas-phase collection, glass tubes are filled with approximately 8.75 cm<sup>3</sup> of resin (held in place using glass wool), which efficiently collects the test compound from the gas flow. In preliminary control tests, we used two XAD tubes in series to test whether any compound bleeds from a single tube. We observed no bleed for guaiacol or guaiacylacetone from the first XAD plug to the second in our longest collection times (90 minutes). Additional delivery tests confirmed that guaiacol deposition amounts on the order of tens of µmol are efficiently trapped in a single plug. Thus, we typically used only one XAD plug for a given experiment. Each time a new compound is tested, corresponding blank and bleed analyses must be performed to ensure no issues with quantitation.

At the end of a given collection time, we remove the XAD trap, pour the XAD resin and glass wool into a 100-mL glass beaker, add 30 mL of acetonitrile, cap the beaker tightly with foil, and shake the beaker for 30 minutes. An accompanying matrix spike is also run with each experiment to determine the percent recovery of the test compound from the resin: an experimentally identical tube of XAD-4 resin and glass wool is emptied into a beaker and a

known mass of test compound (prepared as a solution in acetonitrile) is spiked onto the dry resin and extracted in the same manner as the regular samples. For GUA and GA, average ( $\pm$  1 $\sigma$ ) percent recoveries are 96  $\pm$  9 and 82  $\pm$  7, respectively. All extracts are filtered through 0.05  $\mu$ m syringe filters (Tisch Scientific) and then 350  $\mu$ L of extract is added to 650  $\mu$ L of water to match the mobile phase used for LC-MS analysis.

We validated our system using guaiacol (2-methoxyphenol), a significant component of biomass burning emissions  $^4$  whose Henry's law constant has been measured using both gas stripping and headspace measurement techniques with good agreement  $^5$ . We selected guaiacol for our initial tests since it is quite volatile, which should reveal any system design problems with XAD loading capacity (i.e., if the XAD plugs cannot collect all of the gas-phase guaiacol) or gas flow rate (i.e., if our gas flow rate is too fast to allow equilibrium partitioning in the wetted wall column). As shown in Figure S3,  $K_{\rm H}$  is constant for flow rates between 25 and 600 cm $^3$  min $^{-1}$ , with a value not statistically different from past work  $^5$  based on a t-test for differences in means at 95% confidence. These results indicate that equilibrium is established across the entire range of flow rates and suggest that the less stringent constraint on diffusion distance (i.e., x = 2r from above) is applicable to this system. We set a flow rate of 50 mL min $^{-1}$  for guaiacol tests because this setting strikes a balance between collected gas-phase guaiacol mass (extract concentrations on the order of  $\mu$ M) and experiment run time (longest collection 90 minutes). All guaiacol data here are collected at 298 K and ambient pressure.

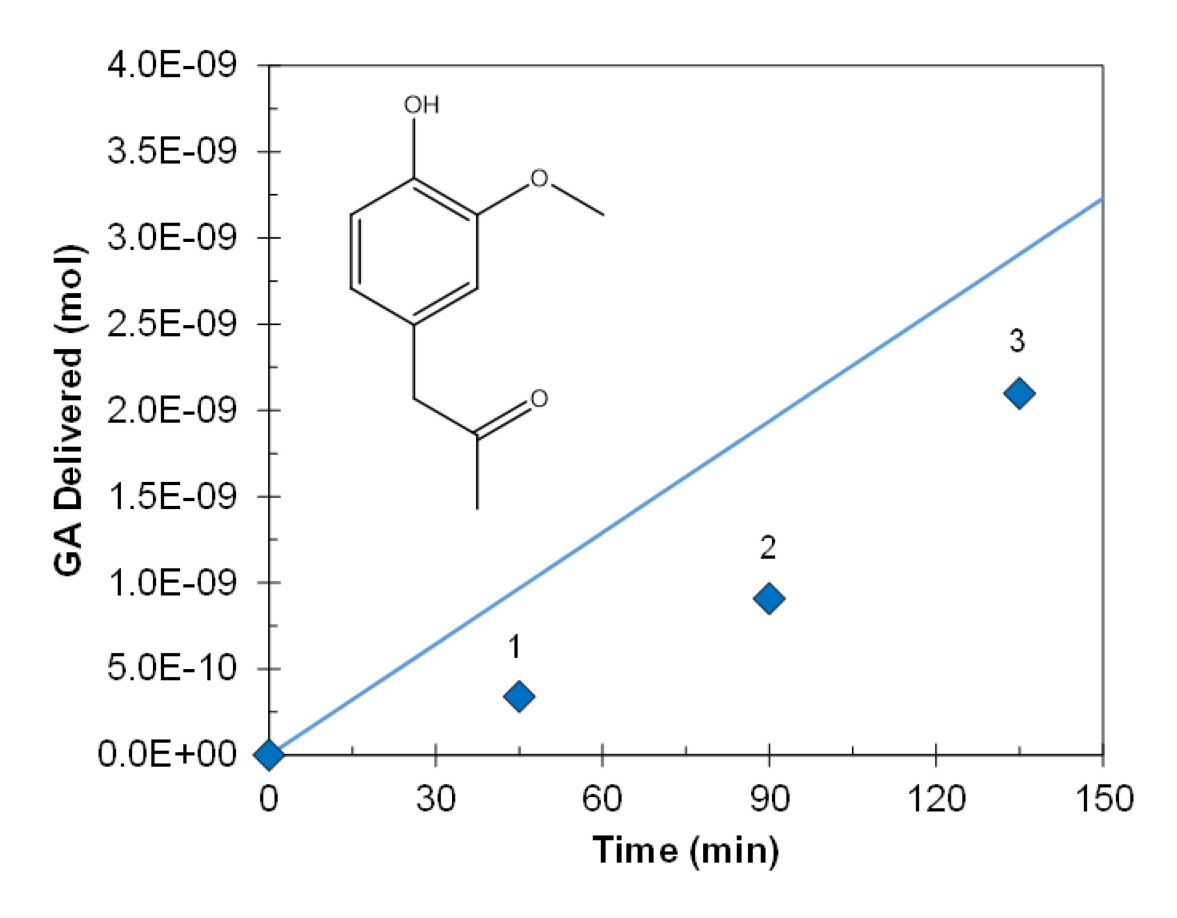


**Figure S2.** The effect of incomplete system conditioning on the  $K_{\rm H}$  determination of guaiacylacetone at 283 K using a reservoir concentration of 18.2 mM. The numbers next to each data point correspond to the sample run order. Initial samples contain lower amounts of compound than expected due to sticking of guaiacylacetone to active sites within the system, with a smaller effect as conditioning time increases. The line shows the delivery of GA in a 283 K experiment with proper system conditioning (reservoir concentration = 12.0 mM).

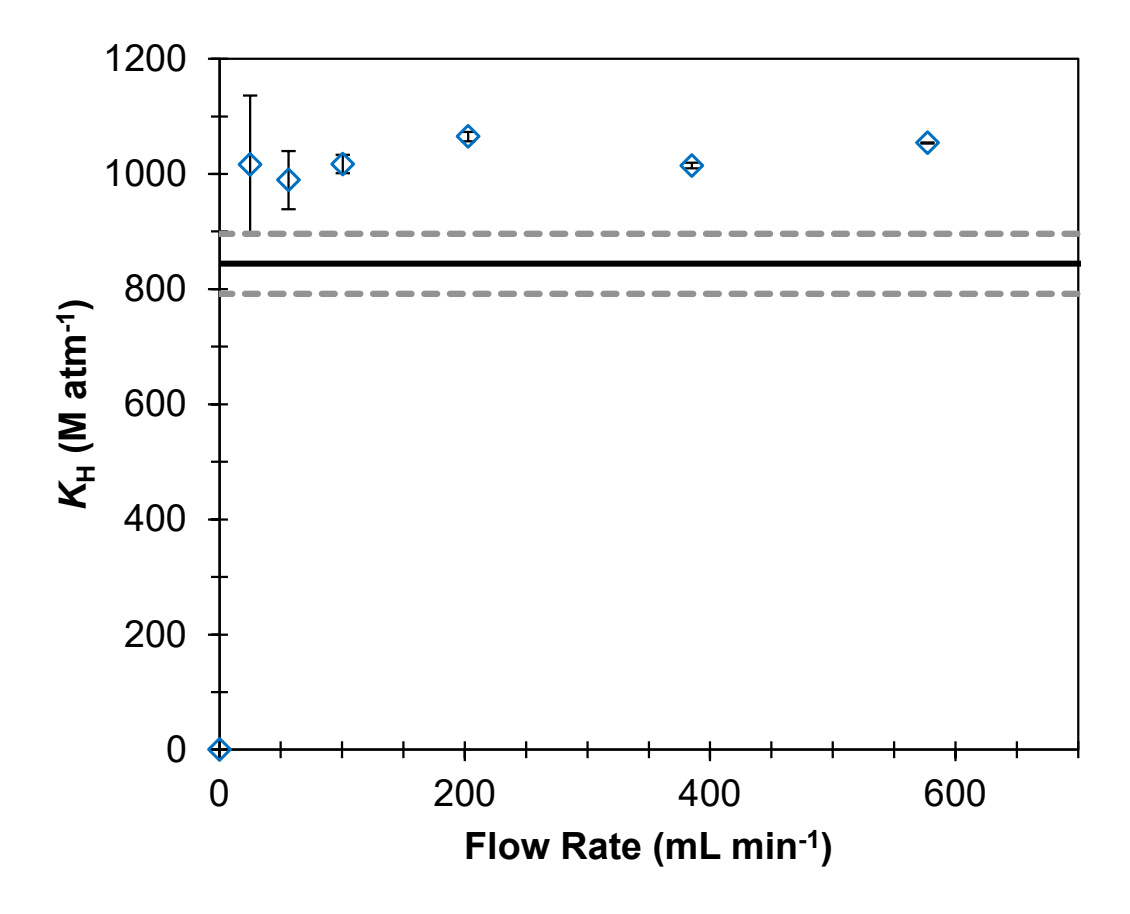


**Figure S3.** Dependence of measured  $K_{\rm H}$  for guaiacol at 298 K on the system gas flow rate. Error bars are the standard errors of each measurement. Each  $K_{\rm H}$  value is determined using a single collection point. The black dotted line and grey dashed lines represent data of Sagebiel et al., and represent the average and standard deviation, respectively.<sup>5</sup>

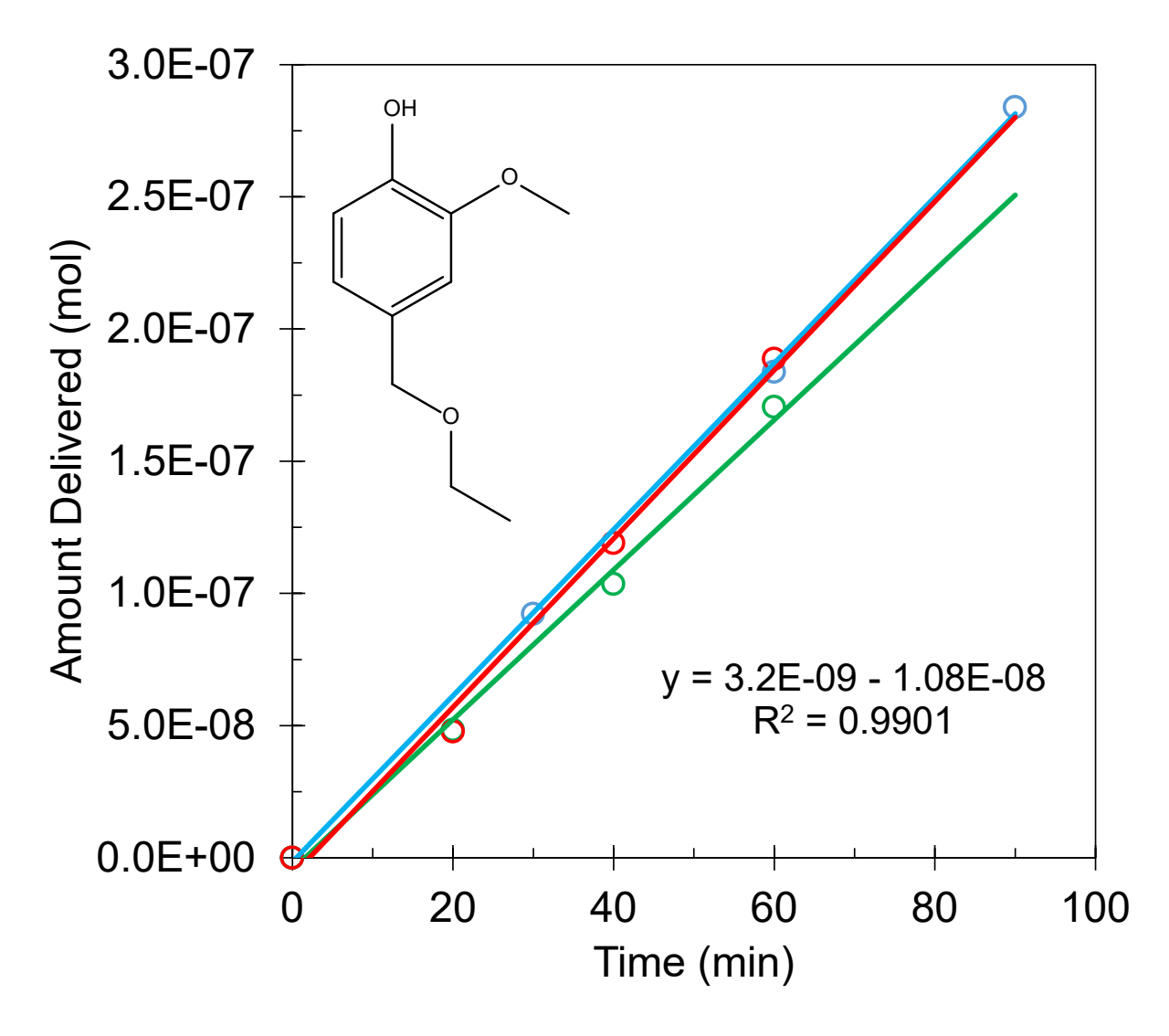


**Figure S4.** Example of generated  $K_H$  data for vanillyl ethyl ether at 298 K. Each symbol color represents one experiment with its corresponding trendline. Samples were run in descending order on each day (e.g., 60-40-20 minute collections). The equation and  $R^2$  value correspond to the average trendline of all data.

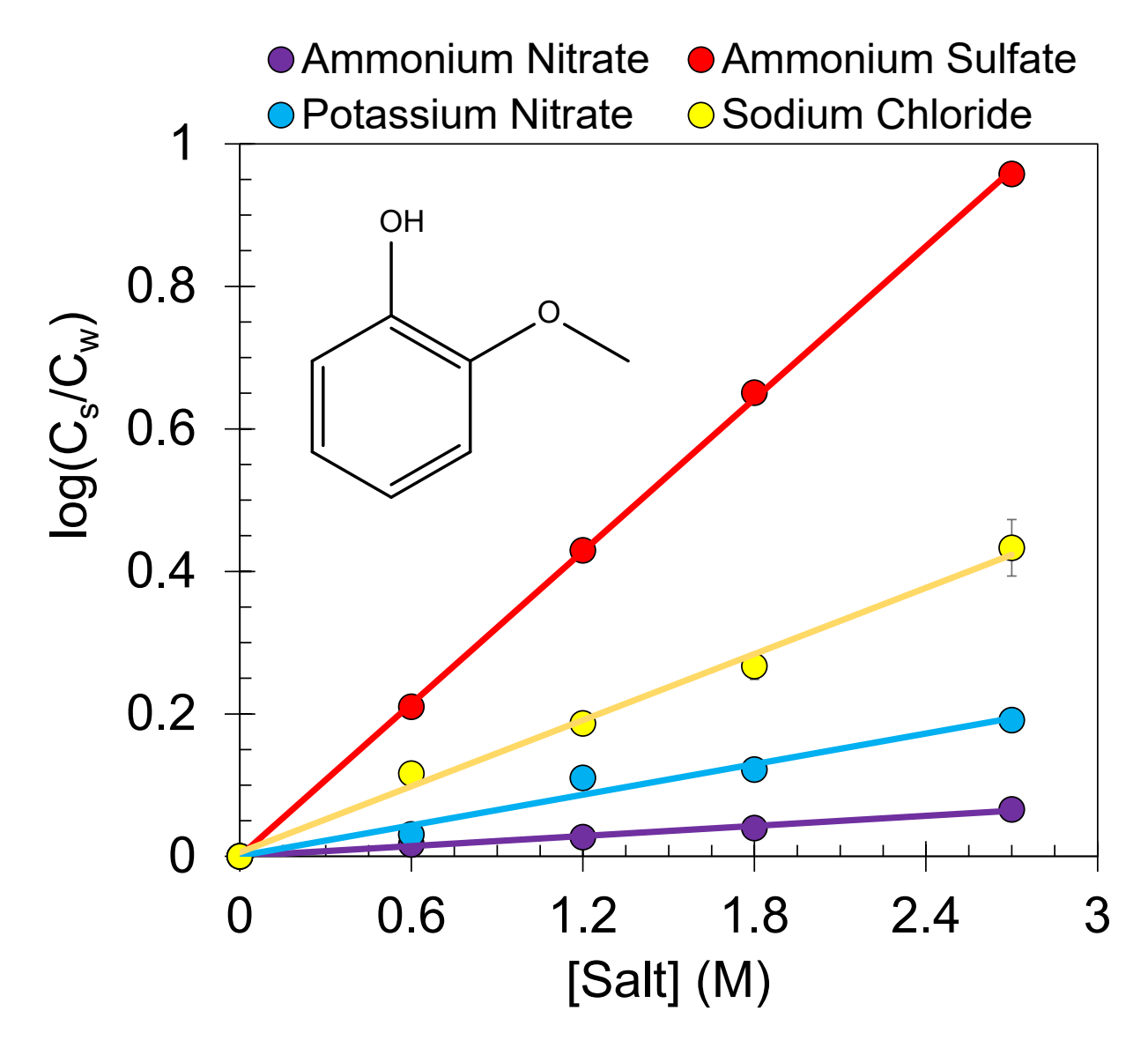


**Figure S5.** Measured  $K_S$  data for guaiacol with four salts, where  $C_S$  and  $C_W$  represent the fiber amounts in salt water and fresh water, respectively. Points are the average of triplicate determinations with error bars representing  $\pm 1\sigma$  about the mean (often too small to observe).

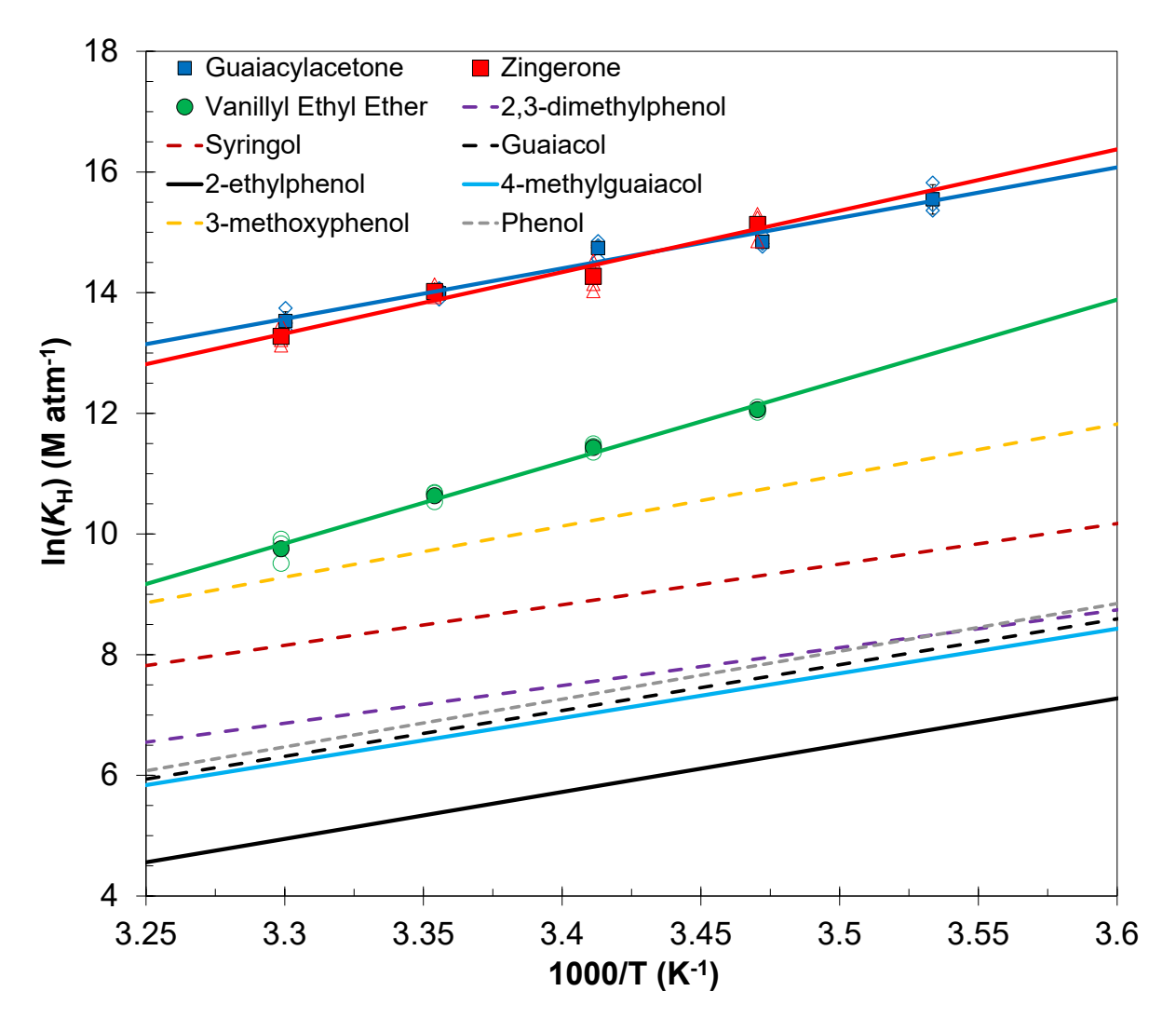


**Figure S6.** Experimentally determined temperature dependences for selected phenols in van't Hoff form. Zingerone (red squares), guaiacylacetone (blue squares), and vanillyl ethyl ether (green circles) values are from this work. Error bars represent  $\pm 1\sigma$  of at least three measurements. Dotted lines represent temperature dependences determined from literature values of  $\Delta H_{\rm sol}$  from Sagebiel et al. (guaiacol, 4-methylguaiacol, syringol),<sup>5</sup> Feigenbrugel et al. (phenol),<sup>6</sup> Dohnal and Fenclova (2,3-dimethylphenol),<sup>7</sup> and Mackay et al. (2-ethylphenol, 3-methoxyphenol).<sup>8</sup>

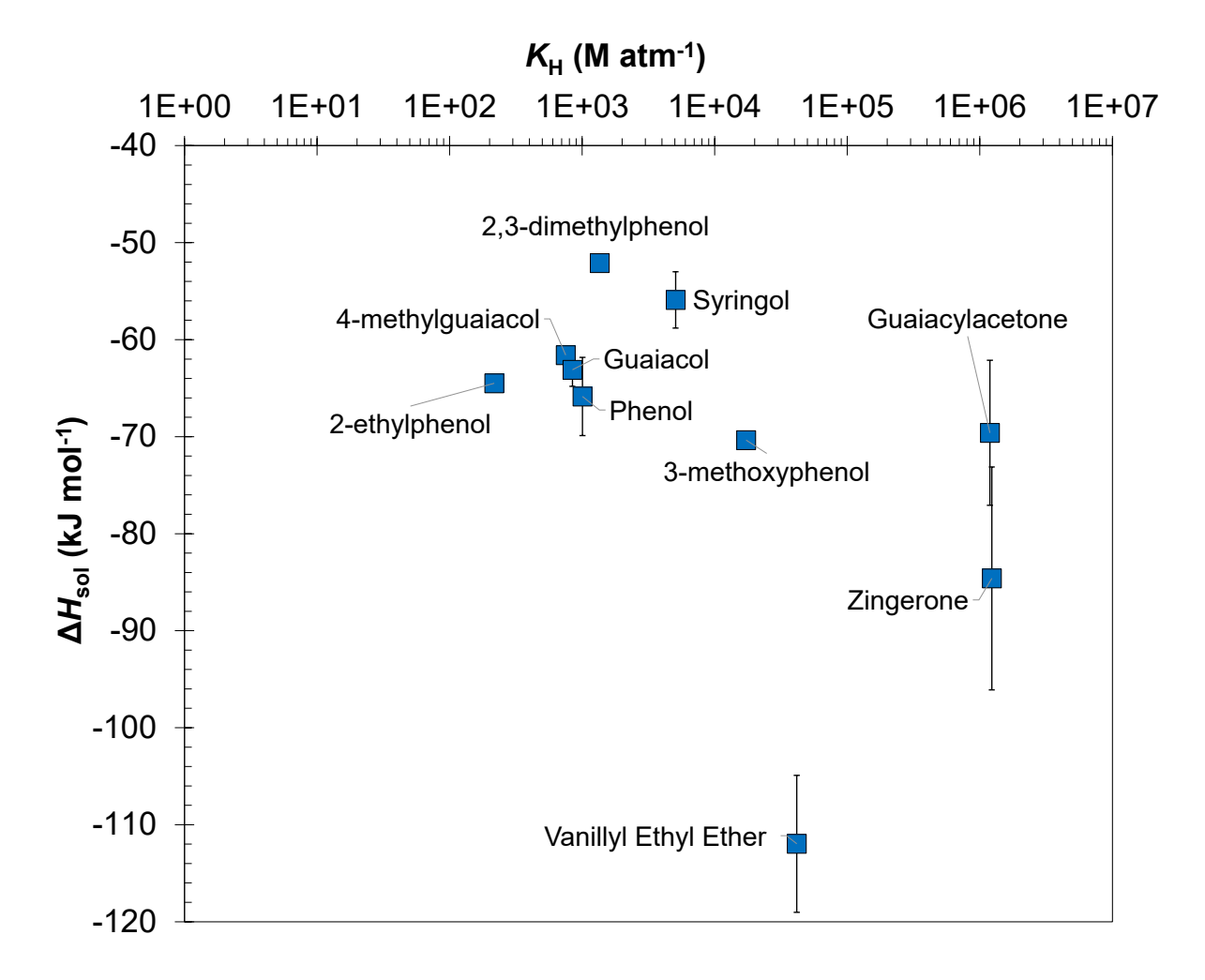


**Figure S7.** Relationship between  $K_{\rm H}$  and  $\Delta H_{\rm sol}$  for phenols. Zingerone, guaiacylacetone, and vanillyl ethyl ether values are from this work. Error bars represent  $\pm 1\sigma$  where available. Other values of  $\Delta H_{\rm sol}$  are from Sagebiel et al. (guaiacol, 4-methylguaiacol, syringol),<sup>5</sup> Feigenbrugel et al. (phenol),<sup>6</sup> Dohnal and Fenclova (2,3-dimethylphenol),<sup>7</sup> and Mackay et al. (2-ethylphenol, 3-methoxyphenol).<sup>8</sup>

**Table S2.** Recoveries from XAD-4 resin for the phenols tested in this work.

Average	SD	Solvent
91.6	6.2	ACN
95.5	8.0	ACN
83.3	6.3	ACN
81.3	9.2	ACN
79.8	6.7	ACN
85.3	5.1	ACN
46.8	10.1	35:65 ACN:H2O
57.2	6.5	35:65 ACN:H2O
	91.6 95.5 83.3 81.3 79.8 85.3 46.8	91.6 6.2 95.5 8.0 83.3 6.3 81.3 9.2 79.8 6.7 85.3 5.1 46.8 10.1

**Table S3a.** ESI (+ mode) and chromatography information for  $K_{\rm H}$  experiments. Eluent ratios are v:v of acetonitrile:water. The column is an Agilent Poroshell 120 PFP column (50 x 2.7 mm). The source capillary voltage was 4000 V.  $T_{\rm R}$  is retention time.

Compound	Frag	CE	CEV	Precursor Ion	Product Ion	Eluent	Flow Rate (mL min <sup>-1</sup> )	T <sub>R</sub> (min)
4-propyl guaiacol	70	7	7	167.1	107	40:60	0.50	1.92
Guaiacol	75	10	5	125	93	35:65	0.50	1.57
Eugenol	70	7	7	165.1	137.1	35:65	0.50	2.15
Vanillyl ethyl ether	75	22	7	137.1	94.1	35:65	0.35	1.65
Guaiacylacetone	100	15	4	181	124.1	35:65	0.35	1.29
Zingerone	100	10	7	195.1	137.1	35:65	0.35	1.53
Vanillyl alcohol	100	15	7	137.1	122.1	40:60	0.50	0.69
Syringylacetone	100	15	7	211.1	137.1	35:65	0.35	1.22

**Table S3b.** ESI (+ mode) segment and chromatography information for *K*s experiments. The eluent was 40:60 acetonitrile:water flowing at 0.7 mL min<sup>-1</sup> through a Thermo Scientific BetaBasic C18 column (250 x 3 mm). ESI settings were identical to Table S2a.

Time Segment Start (min)	<b>Analyzed Compounds</b>	T <sub>R</sub> (min)
0	To Waste	
1.75	VanOH	2.06
2.4	SA, GA, Zing, Gua	2.60, 2.75, 3.23, 3.56
3.75	VanEth	3.95
7	Eug	7.94
9	PropGua	11.09

Table S4. EPI Suite estimated and measured Henry's law constants (units M atm<sup>-1</sup>).

Measured Values		<b>EPI Suite Est</b>	timates of K <sub>H</sub>	Ratio EPI:Measured		
Compound	$K_{\mathrm{H}}$	SD	<b>Bond Method</b>	<b>EVA Method</b>	<b>Bond Method</b>	<b>EVA Method</b>
4-propyl guaiacol	4.40E+02	2.99E+01	2.06E+04	4.29E+02	47	0.98 a
Guaiacol	8.73E+02	7.70E+01	1.87E+03	8.33E+02	2.1	0.95
Eugenol	9.29E+02	1.26E+01	2.62E+05	5.75E+02	280	0.62 a
Vanillyl ethyl ether	4.15E+04	3.36E+03	1.15E+06	4.85E+04	28	1.2 a
Guaiacylacetone	1.19E+06	1.11E+05	4.10E+07	1.12E+06	34	$0.94^{a}$
Zingerone	1.23E+06	1.19E+05	8.50E+06	8.47E+05	6.9	0.69 a
Vanillyl alcohol	9.69E+06	7.15E+05	2.15E+08	2.06E+07	22	2.1 <sup>b</sup>
Syringylacetone	1.24E+08	1.22E+07	6.90E+08	5.81E+06	5.6	$0.05^{\rm c}$

<sup>&</sup>lt;sup>a</sup> Guaiacol as reference

220

<sup>&</sup>lt;sup>b</sup> 4-methylguaiacol as reference

<sup>&</sup>lt;sup>c</sup> Syringol as reference

**Table S5.** Measured Setschenow coefficients for each salt and phenol (units M<sup>-1</sup>). "Salt Average" reports the value of *K*s averaged across all tested phenols. Tests were conducted at 298 K (though *K*s is independent of temperature).

	(NH	$_{4})_{2}SO_{4}$	N	aCl	NH	I <sub>4</sub> Cl	K	$NO_3$	NH	$_{1}NO_{3}$
Compound	$K_{\rm S}$	SE	$K_{\rm S}$	SE	$K_{\rm S}$	SE	$K_{\rm S}$	SE	$K_{\rm S}$	SE
4-propylguaiacol	0.46	0.026	0.23	0.013	0.14	0.012	0.14	0.014	0.047	0.011
Guaiacol	0.36	0.0079	0.15	0.010	0.062	0.0055	0.071	0.0081	0.023	0.0043
Eugenol	0.40	0.0074	0.19	0.0052	0.10	0.0054	0.10	0.0044	0.053	0.0049
Vanillyl Ethyl Ether	0.56	0.0070	0.23	0.0055	0.12	0.0069	0.13	0.0043	0.062	0.0036
Guaiacylacetone	0.51	0.048	0.25	0.016	0.15	0.013	0.10	0.018	0.022	0.011
Zingerone	0.57	0.020	0.24	0.0073	0.085	0.0051	0.086	0.0071	0.019	0.0043
Vanillyl Alcohol	0.37	0.0066	0.14	0.0070	0.051	0.0047	0.062	0.0078	0.034	0.0070
Syringylacetone	0.65	0.071	0.34	0.012	0.17	0.013	0.11	0.015	0.044	0.015
Salt Average $\pm \sigma$	0.49	± 0.11	0.22 =	± 0.063	0.11 ±	- 0.044	0.10 ±	- 0.028	0.038	± 0.016

**Table S6.** Tabulated  $K_{\rm H}$  constants and  $\Delta H_{\rm sol}$  values for woodsmoke phenols identified in Schauer et al.<sup>4</sup> Superscipt source numbers correspond to the literature reference for measured data. Asterisks denote data reported from a QSAR or other non-experimental approach.

230

Compound	Physical K <sub>H</sub> at 298 K (M atm <sup>-1</sup> )	Source	EVA Ref Compound	ΔH <sub>sol</sub> (kJ mol <sup>-1</sup> )	
phenol and substituted phenols					
benzaldehyde	4.0E+01	Measured <sup>10</sup>		-39.9	
o-cresol	8.3E+02	Measured <sup>6</sup>		-60.7	
m-cresol	1.0E+03	Measured <sup>6</sup>		-59.9	
2,4-dimethylphenol	1.1E+03	Measured <sup>7</sup>		-54.9	
p-cresol	1.3E+03	Measured <sup>6</sup>		-59.9	
phenol	5.0E+02	Measured <sup>6</sup>		-65.8	
o-benzenediol	4.7E+03	Measured <sup>8</sup>		-52.4	
p-methoxybenzaldehyde	7.0E+03	Measured <sup>11</sup>		-70.2	
o-methoxybenzaldehyde	1.8E+04	Measured <sup>11</sup>		-71.7	
m-methoxybenzaldehyde	3.5E+04	Measured <sup>11</sup>		-70.5	
2-hydroxybenzaldehyde	4.1E+05	EVA Method	3-hydroxybenzaldehyde		
3-hydroxybenzaldehyde	4.1E+05	Measured <sup>12</sup> *		-71.5	
4-hydroxybenzaldehyde	1.9E+06	Measured <sup>12</sup> *		-71.5	
m-benzenediol	8.4E+06	Measured <sup>8</sup>		-52.4	
p-benzenediol	2.3E+07	Measured <sup>8</sup>		-52.4	
tyrosol	3.5E+07	EVA Method	4-ethylphenol		
guaiacol and substituted guaiacols					

4-propylguaiacol	4.4E+02	This Work		
4-ethylguaiacol	5.6E+02	EVA Method	4-methylguaiacol	
4-methylguaiacol	7.3E+02	Measured <sup>5</sup>		-61.5
guaiacol	8.7E+02	This Work		-62.4
eugenol	9.3E+02	This Work		
cis-isoeugenol	1.7E+03	EVA Method	eugenol	
trans-isoeugenol	1.7E+03	EVA Method	eugenol	
vanillyl ethyl ether	4.2E+04	This Work		-112.2
vanillin	4.7E+05	Measured <sup>13</sup>		
acetovanillone	6.4E+05	EVA Method	vanillin	
guaiacyl acetone	1.2E+06	This Work		-69.8
zingerone	1.2E+06	This Work		-84.8
coniferylaldehyde	4.5E+06	EVA Method	eugenol	
vanillyl alcohol	9.7E+06	This Work		
syringol and substituted syringols				
4-propylsyringol	2.2E+03	EVA Method	syringol	
4-ethylsyringol	3.0E+03	EVA Method	syringol	
4-methylsyringol	3.9E+03	EVA Method	syringol	
syringol	5.0E+03	Measured <sup>5</sup>		-55.7
allylsyringol	6.4E+04	EVA Method	syringyl acetone	
4-propenylsyringol	1.1E+05	EVA Method	syringyl acetone	
butyrylsyringol	2.9E+07	EVA Method	syringyl acetone	
syringaldehyde	3.7E+07	EVA Method	syringyl acetone	
propionylsyringol	3.8E+07	EVA Method	syringyl acetone	
acetosyringone	5.1E+07	EVA Method	syringyl acetone	
syringyl acetone	1.2E+08	This Work		
sinapylaldehyde	3.1E+08	EVA Method	syringyl acetone	

## References

- 1. Mozurkewich, M., Mechanisms for the release of halogens from sea-salt particles by free radical reactions. *Journal of Geophysical Research: Atmospheres* **1995**, *100*, (D7), 14199-14207.
- 237 2. Friedlander, S. K., *Smoke, Dust and Haze: Fundamentals of Aerosol Behavior*. 2 ed.; Oxford University Press: New York, 2000; p 407.
- 3. EPA, U. S. *Estimation Programs Interface Suite™ for Microsoft® Windows*, v 4.11; United States Environmental Protection Agency: Washington, DC, USA, 2012.
- Schauer, J. J.; Kleeman, M. J.; Cass, G. R.; Simoneit, B. R. T., Measurement of Emissions from Air Pollution Sources.
   C1-C29 Organic Compounds from Fireplace Combustion of Wood. *Environmental Science & Technology* 2001, 35, (9), 1716-1728.
- 5. Sagebiel, J. C.; Seiber, J. N.; Woodrow, J. E., Comparison of headspace and gas-stripping methods for determining the Henry's law constant (H) for organic compounds of low to intermediate H. *Chemosphere* **1992**, *25*, (12), 1763-1768.
- 6. Feigenbrugel, V.; Le Calvé, S.; Mirabel, P.; Louis, F., Henry's law constant measurements for phenol, o-, m-, and p-cresol as a function of temperature. *Atmospheric Environment* **2004**, 38, (33), 5577-5588.
- Dohnal, V.; Fenclova, D., Air-water partitioning and aqueous solubility of phenols. *Journal of Chemical and Engineering Data* 1995, 40, (2), 478-483.
- 8. Mackay, D.; Shiu, W.-Y.; Lee, S. C., *Handbook of physical-chemical properties and environmental fate for organic chemicals*. CRC press: 2006.
- 9. May, W. E.; Wasik, S. P.; Freeman, D. H., Determination of the solubility behavior of some polycyclic aromatic hydrocarbons in water. *Analytical Chemistry* **1978**, *50*, (7), 997-1000.
- 10. Betterton, E. A.; Hoffmann, M. R., Henry's law constants of some environmentally important aldehydes. *Environmental Science & Technology* **1988**, *22*, (12), 1415-1418.
- 258 11. Ji, C.; Day, S. E.; Ortega, S. A.; Beall, G. W., Henry's Law Constants of Some Aromatic
   259 Aldehydes and Ketones Measured by an Internal Standard Method. *Journal of Chemical & Engineering Data* 2008, 53, (5), 1093-1097.
- 12. Nirmalakhandan, N.; Brennan, R. A.; Speece, R., Predicting Henry's law constant and the effect of temperature on Henry's law constant. *Water Research* **1997**, *31*, (6), 1471-1481.
- 263 13. Yaws, C., Handbook of vapor pressure, Gulf Pub. Co., Houston 1994.